A Diagnostic Study of Three Heavy Precipitation Episodes in the Western Mediterranean Region

CHARLES A. DOSWELL III

NOAA/Environmental Research Laboratories, National Severe Storms Laboratory, Norman, Oklahoma

CLEMENTE RAMIS, ROMUALDO ROMERO, AND SERGIO ALONSO

Geophysical Fluid Dynamics Group, University of the Balearic Isles, Palma de Mallorca, Spain

(Manuscript received 21 May 1996, in final form 3 November 1997)

ABSTRACT

A diagnostic evaluation of three project ANOMALIA case studies involving heavy precipitation in the western Mediterranean region has been carried out. The evaluation shows the unique characteristics of each event, as well as some limited similarities. Heavy precipitation events in the western Mediterranean region typically occur downstream of a significant cyclone aloft (often, but not always, exhibiting ''cutoff'' cyclone characteristics), but important structural and evolutionary differences are found among these cases. At low levels, a long fetch of flow over the Mediterranean Sea frequently interacts with terrain features to produce persistent heavy precipitation. Although most heavy precipitation events occur during the fall season, they can develop at other times. In the first case, the synoptic-scale environment produced low static stability and substantial storm-relative environmental helicity, thereby supporting both heavy rain in the vicinity of Valencia on mainland Spain and on Ibiza in the Balearic Islands, as well as a tornado at Menorca in the Balearic Islands on 7–9 October 1992. The second case involved a slow-moving cyclone that destabilized the stratification and produced several days of heavy precipitation over the period 31 January–6 February 1993. In the third case, in the Italian Piedmont region on 5–6 November 1994, the heavy precipitation included a nonconvective component, with moist but relatively stable air impinging on steep terrain gradients.

A set of basic diagnostic tools is applied to the cases, and it is shown that anything but a superficial diagnosis of each case requires flexibility in selecting diagnostic tools. The ways by which heavy precipitation is created can vary substantially from case to case and in different parts of the world; however, there is a common thread. Heavy precipitation is the result of moist, low-level air ascending rapidly, so any diagnosis aimed at forecasting heavy precipitation needs to address the following: vertical motion, static stability, moisture supply, and orographic effects (when appropriate). Forecasting implications of the cases are discussed, with the emphasis on considering these physically relevant processes.

1. Introduction

Heavy precipitation has the potential to become hazardous virtually anywhere in the world, as witnessed by killer flash flood events recently in such diverse locations as mainland Spain (late November 1995 and again in November 1996), South Africa (January/February 1996), and North Korea (September 1995). It is arguably the most ubiquitous of hazardous weather phenomena, a potential weather disaster across most of the world's populated regions. Any investigation of the processes by which heavy precipitation occurs can be of value to weather forecasters, provided the study focuses on the *physical processes giving rise to the intense precipitation.*

This study considers three cases selected from the set of five ANOMALIA Project[1] events selected by all the ANOMALIA participants as primary cases of particular interest in the western Mediterranean (out of a group of

Corresponding author address: Dr. Charles A. Doswell III, National Severe Storms Laboratory, 1313 Halley Circle, Norman, OK 73069.
E-mail: doswell@nssl.noaa.gov

[1] ANOMALIA's name is derived from the Spanish word for ''anomaly;'' and its stated primary scientific objective is ''to increase the degree of understanding of the non-linear interaction processes taking place as a consequence of the close proximity of mountains and sea that characterizes the western Mediterranean area . . . .'' The ultimate goal of the project is ''an improvement of meteorological models and, as a consequence, of short-range weather forecasts of mesoscale systems that cause severe storms and floods.'' The project was a collaborative effort among several nations of the European Union and officially ended in spring of 1997. The design and objectives of the ANOMALIA project are described in an unpublished contract agreement for the project between the participating institutions and the European Community (EC).

© 1998 American Meteorological Society

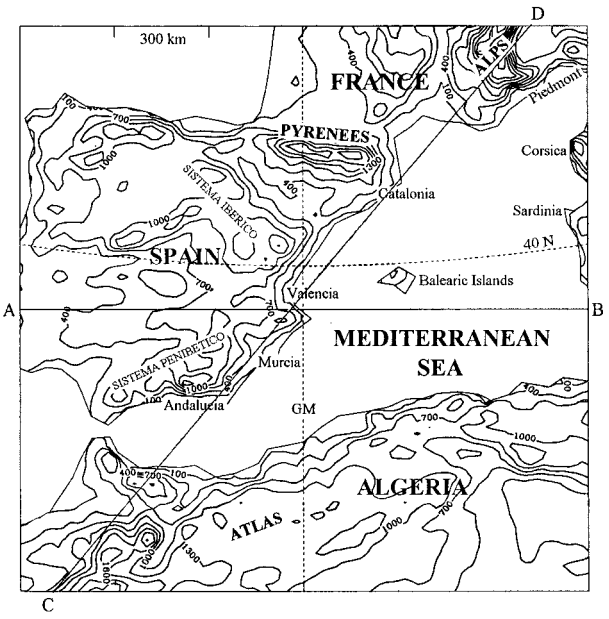

FIG. 1. Map of the western Mediterranean region, showing major topographic features by means of terrain contours (interval 300 m, starting at 100 m), names of locations mentioned in the text, and the lines AB and CD, which depict cross sections discussed in the text.

roughly 20 candidate events). These three cases were chosen for study because they involved diverse heavy precipitation events in the western Mediterranean.

The western portion of the Mediterranean Sea (Fig. 1) is that area enclosed by Spain, France, Corsica, Sardinia, northwestern Italy, Africa, and lands nearby (Meteorological Office 1962). This region frequently is affected by heavy convective rain, especially during autumn. Along the Spanish Mediterranean coast there are many examples of high precipitation rates; for examples, see García-Dana et al. (1982), Benet (1986), Font (1983), Fernández et al. (1995), and Ramis et al. (1995). Riosalido (1990) has shown that most of the heavy rainfall events in the western Mediterranean region can be attributed to mesoscale convective systems, although they typically are relatively small in size and practically never fulfill the criteria for a mesoscale convective complex given by Maddox (1980). The majority of heavy rainfall in the region is convective in character, but convection is not dominant in *every* case, as we shall show.

The western Mediterranean area has unique geographical aspects that can dominate local weather events. Figure 1 shows several topographic features of interest, as well as providing locations of specific sites mentioned in this paper. Notable among the topographic features are the Mediterranean Sea itself and the region's orography, including the Atlas Mountains of northwestern Africa, several mountain ranges in mainland Spain (e.g., Sistema Ibérico and Sistema Penibético), the Pyrenees, and the western portion of the Alps. These topographic features play a large role in the structure and evolution of the weather systems associated with heavy precipitation.

This paper explores three of the ANOMALIA cases with the intent to provide overview descriptions of the events for weather forecasters in the western Mediterranean. We also hope to use these examples to demonstrate the application of some basic principles for diagnosis of threatening weather situations anywhere in the world, particularly those involving severe storms and heavy precipitation. The approach focuses on synoptic-scale processes and parameters most directly and unambiguously related to the occurrence of heavy precipitation. Mesoscale details are not resolved in the data but can sometimes be inferred from a knowledge of the interaction between synoptic-scale processes and the topography. The diagnostic concept used has been developed at some length in Doswell et al. (1996) and is consistent with previous studies of heavy precipitation in the western Mediterranean region (see, e.g., Ramis et al. 1994).

In section 2 of this paper, we describe the data used for diagnosing events, as well as the diagnostic tools to be employed in this work. Section 3 reviews the synoptic situation for each event, with the intent being to emphasize both the similarities and the differences among the three cases. The focus is on those processes that we believe contributed to heavy precipitation as revealed by the diagnoses. Section 4 concludes the paper with a discussion based on our interpretation of the three cases, emphasizing the possible forecasting implications.

2. Data and diagnostic methodology

Most of the data used in this analysis are from the European Centre for Medium-Range Weather Forecasts (hereinafter ECMWF). The data are provided on a 0.75° latitude–longitude grid at standard pressure levels. These gridded data are the initial fields used in the ECMWF numerical model forecasts.[2] Since these data are specified on a grid at a fixed number of levels, some smoothing of the details contained in the original data is expected. An example of the relationship between the raw observations and the gridded data is shown in Fig. 2, for the sounding site at Palma de Mallorca in the Balearic Isles (see Fig. 1) at 1200 UTC 8 October 1992. The original data contain considerably more detail in the vertical, as might be expected, in comparison to the limited number of levels in the model, but the gridded data appear to be broadly similar to the observations. What these data are suited for is diagnosis of the syn-

[2] The basics of the data assimilation scheme are described in Hollingsworth et al. (1986) but the details change over time, as noted by Trenberth and Olson (1988). It employs a so-called optimal interpolation of the new observational data, using a recent forecast as the initial guess.

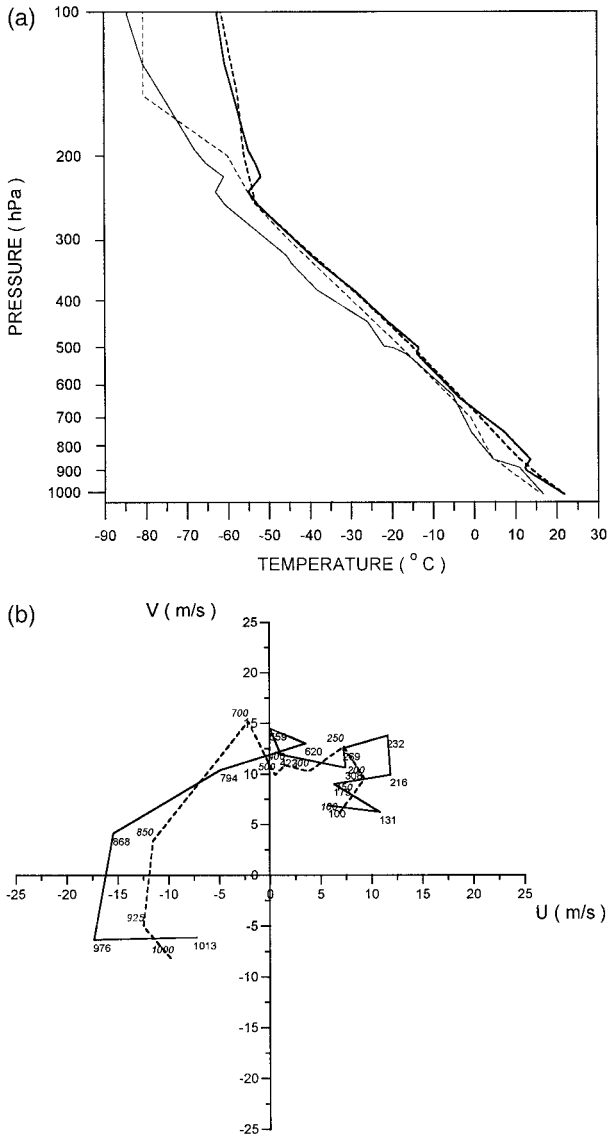

FIG. 2. Comparison of the vertical atmospheric structure deduced from radiosonde ascent (solid lines) in Palma (Balearic Islands), and the nearest grid point to Palma from the ECMWF data (dashed lines) at 1200 UTC 8 October 1992: (a) temperature and dewpoint, (b) hodograph, with labels indicating pressure levels.

optic-scale aspects of each situation, and that capability matches our interests in this study.

There are at least two major advantages to using these as our primary data. First, the data have been defined on a computational grid, thereby removing the need to do additional ''objective analysis'' in order to carry out diagnostic computations. Second, over the data-void regions (notably, over the Mediterranean Sea), combining a forecast model's ''first guess'' with the limited observations provides a reasonable estimate of the field values, whereas an analysis based only on the raw observations would necessarily have problems in any data-sparse regions (Buzzi et al. 1991).

Observed rainfall data for the first two cases are from the Instituto Nacional de Meteorología of Spain (INM); in the third case, rainfall observations were provided by Institute of Physics and Chemistry of the Lower and Upper Atmosphere (FISBAT) in Bologna, Italy. An example of the spatial density of the rainfall observations in Spain is given in Fig. 3. In Spain, these observations are only available as 24-h totals, and so it is not possible to determine from them at what time within the 24-h period the rainfalls were concentrated. This poses a difficulty for our synoptic-scale overviews only in our second case, in Spain, because the rainfall apparently overlaps the time separating 24-h totals. For the third case in Italy, although hourly data are available, the 24-h totals have been deemed sufficient for our overview purposes.

What is required for deep, moist convection is the existence of sufficient moisture and steep enough lapse rates for low-level parcels to become buoyant when lifted. The diagnosis emphasizes the spatial and temporal distribution of the mechanisms that at synoptic scales favor the development of convection. Caracena and Fritsch (1983) and Doswell (1987), among others, point out that the identification of upward motion areas at synoptic scale using quasigeostrophic theory can provide important guidance in determining development zones of convective storms. Also, Barnes (1985) and Durran and Snellman (1987) show that the analysis of quasigeostrophic forcing of vertical motion can provide short-term guidance for the prediction of convective events.

The right-hand side of the ω equation (denoted by FQ) has been calculated on isobaric surfaces using a **Q**-vector formulation (see Hoskins and Pedder 1980):

$$\mathrm{FQ} = -2\frac{R}{p}\nabla\cdot\mathbf{Q}.$$

The **Q** vector is given by

$$\mathbf{Q} = \nabla\mathbf{V}_g\cdot\nabla T,$$

where R is the dry air constant, p the pressure, $\mathbf{V}_g$ the geostrophic wind, and T the temperature. The quantitative *response* to the forcing term (i.e., ω) requires solution of the ω equation (an elliptic partial differential equation), and is dependent on the static stability (weak stability implies a greater response to a given amount of forcing than when the stability is large) and the boundary conditions chosen. Durran and Snellman (1987) provide an excellent physical discussion of the relationship between quasigeostrophic ω and FQ, suggesting that FQ and ω need not coincide exactly. When FQ has some vertical consistency, however, it is plausible to assume a broad qualitative correspondence between FQ and ω.

Surface moisture flux convergence combines two of the three ingredients for deep, moist convection by identifying subsynoptic-scale regions (i.e., identifiable in surface data) of upward motion in the presence of low-

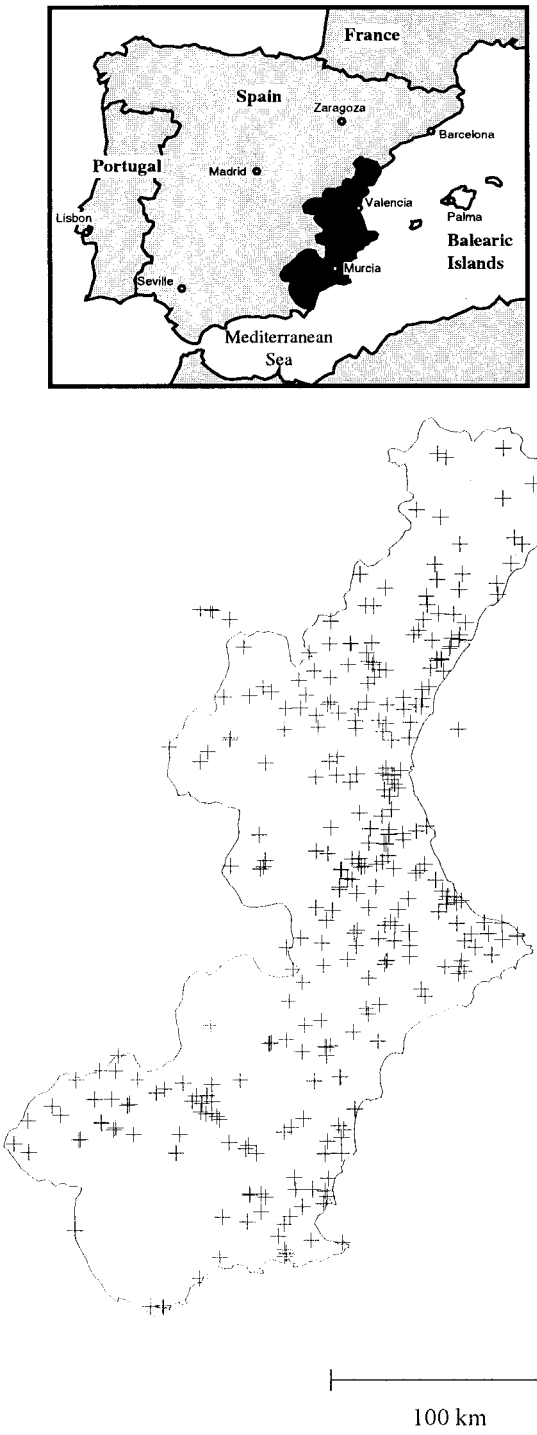

FIG. 3. Rainfall observation sites (crosses) available in the Valencia and Murcia regions of Spain (see inset for location). This distribution of sites is typical of the western Mediterranean region.

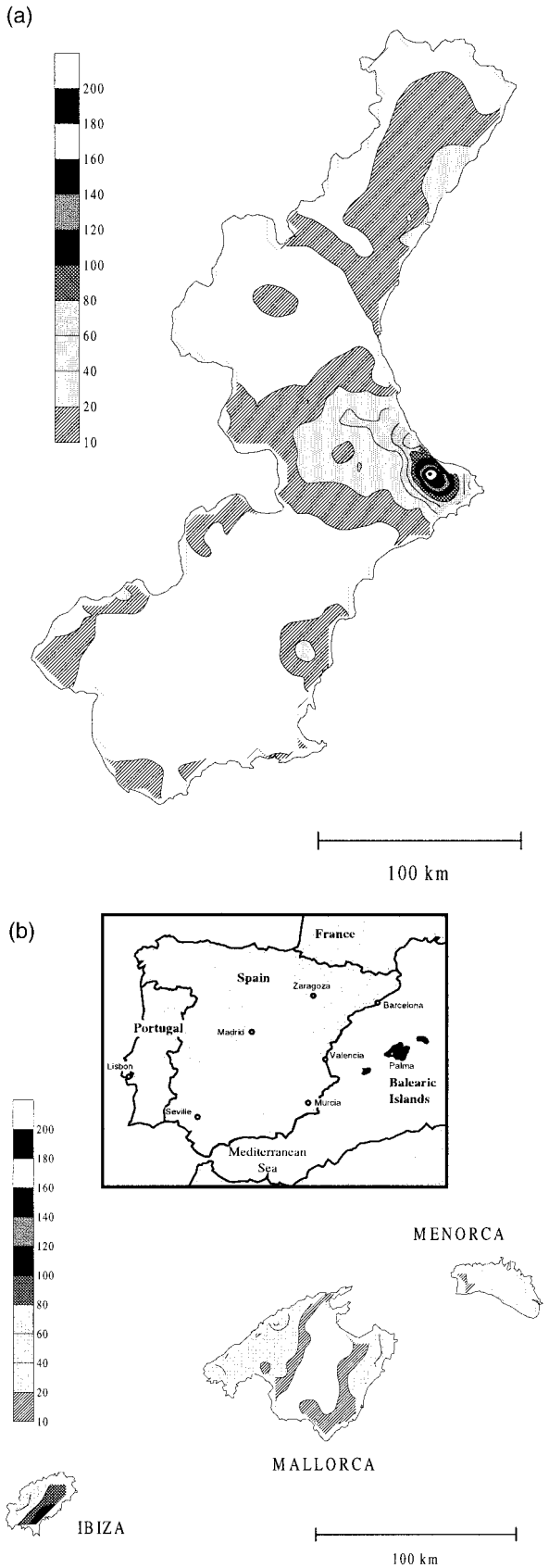

FIG. 4. Accumulated 24-h rainfall in mm, for the period from 0700 UTC 8 October 1992 to 0700 UTC 9 October 1992: (a) Valencia and Murcia regions (see inset from Fig. 3), (b) Balearic Islands (see inset).

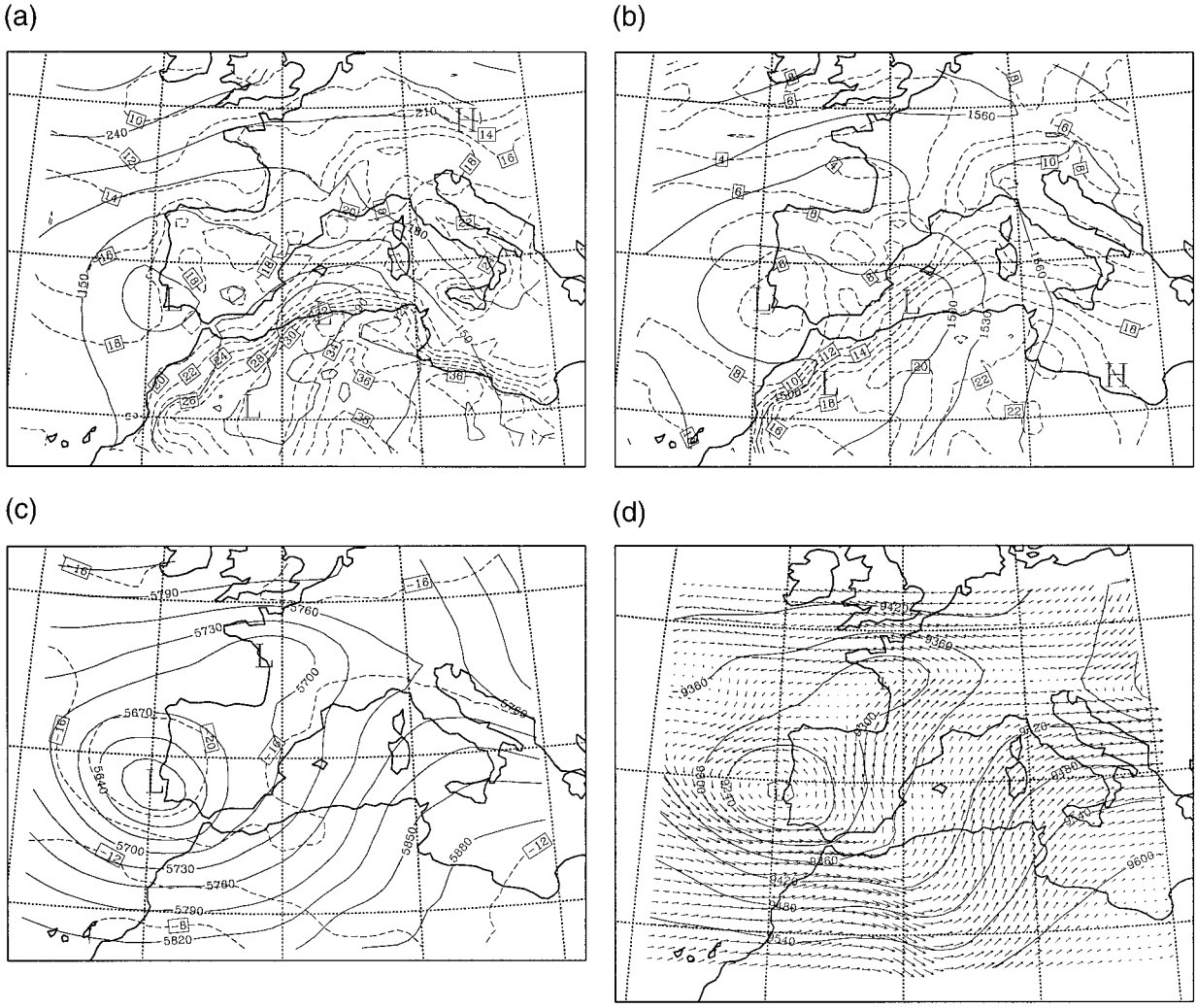

FIG. 5. Meteorological situation at 1200 UTC 8 October 1992 from ECMWF data: (a) 1000, (b) 850, (c) 500, and (d) 300 hPa. Isohypses (dam) and isotherms (°C) for (a), (b), and (c); isohypses and wind vectors for (d). Arrow in the upper-right corner of (d) represents 50 m s^{-1}.

level moisture (Barnes and Newton 1986). As noted in Doswell et al. (1996), heavy rainfall requires the rapid ascent of moist air, and low-level moisture convergence has demonstrated its utility in diagnosing subsynoptic-scale regions favoring convection for just this reason. The water vapor flux divergence is calculated using

$$F_w = -\int_{p_o}^{p} \nabla\cdot(q\mathbf{V})\frac{dp}{g},$$

where q is the specific humidity, p_o is 1000 hPa, and $\mathbf{V}$ is the horizontal wind. In most cases, the contribution to F_w from the divergence dominates the advective contribution. Therefore, computation of F_w is sensitive to the normal difficulties in calculating horizontal divergence of the wind.

We have diagnosed equivalent potential temperature (θ_e), calculated using Bolton's (1980) formula; this variable combines temperature and humidity into a single measure that determines which moist adiabat a parcel will ascend, using parcel theory. In some cases, it is useful to consider moisture and static stability separately, however. Mixing ratio r is a widely used measure of low-level moisture content. For static stability, a simple measure is found by taking the temperature difference between 850 and 500 hPa, and dividing by the thickness of the layer.

We also consider the convective available potential energy (CAPE) as another measure of potential buoyancy. By using the vertical gridpoint stack at each grid point as a sounding, CAPE has been calculated using the expression (Weisman and Klemp 1986)

$$\text{CAPE} = g\int_{\text{LFC}}^{\text{EL}} \left(\frac{\theta - \overline{\theta}}{\overline{\theta}}\right) dz,$$

where θ is the potential temperature of the rising parcel,

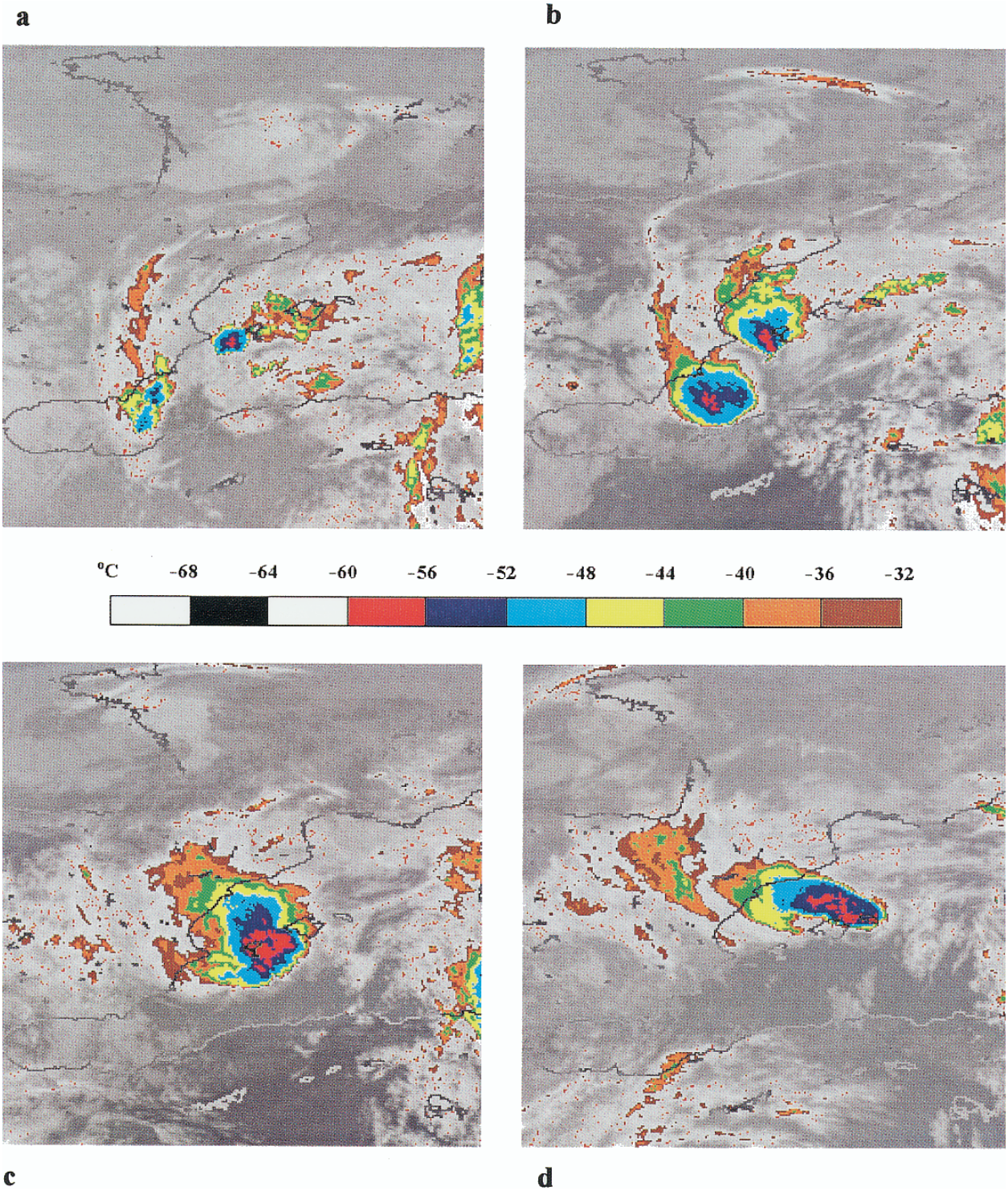

FIG. 6. Meteosat infrared (IR) images on 8 October 1992 at (a) 0500, (b) 1000, (c) 1500, and (d) 2000 UTC.

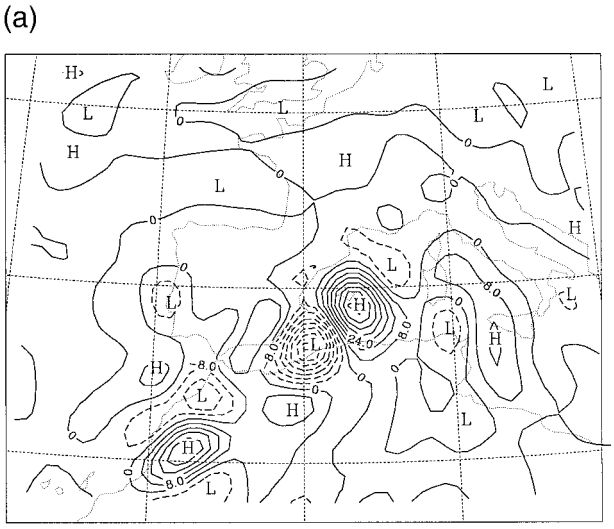

FIG. 7. Quasigeostrophic vertical forcing, FQ (solid lines upward, dashed lines downward), at 1200 UTC 8 October 1992 (a) at 850 and (b) at 500 hPa; isopleth interval is 8×10^{-18} m kg^{-1} s^{-1}.

$\overline{\theta}$ is the potential temperature of the environment, and LFC and EL are, respectively, the level of free convection and the equilibrium level for the rising parcel. The parcel used in the calculations is the surface parcel, which in the western Mediterranean region is almost always the most buoyant parcel in the sounding (Tudurí and Ramis 1997).

For this study, we also consider the storm-relative helicity of the environment. Strictly speaking, storm-relative helicity (SRH) is not a necessary factor in production of heavy rainfall, being more closely associated with tornadoes and supercell convection than rainfall. However, as noted by Doswell (1994), supercells are occasionally quite capable of producing heavy precipitation. The diagnosis of SRH is included in this study since it appears that one of our cases involved supercells. Therefore, SRH has been calculated using the expression (Davies-Jones et al. 1990)

$$\text{SRH} = -\int_0^{z_o} \mathbf{k} \times (\mathbf{V} - \mathbf{C}) \cdot \frac{\partial \mathbf{V}}{\partial z}\, dz,$$

where $\mathbf{C}$ is the storm velocity and z_o is 3000 m. As with CAPE, the vertical stack of gridded data at each grid point in the horizontal has been treated as if it were a sounding.

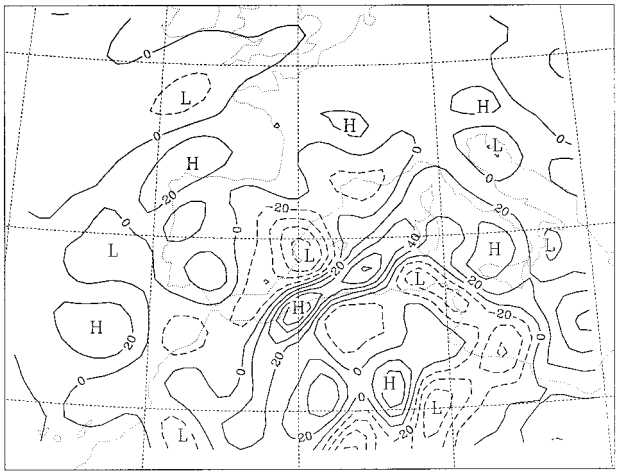

FIG. 8. Divergence (solid lines) and convergence (dashed lines) of water vapor flux in the layer 1000–850 hPa at 1200 UTC 8 October 1992; the isopleth interval is 20 g m^{-2} s^{-1}.

In order to address some issues related to the orographic effects on the flow, we have calculated a Froude number, Fr, defined by

$$\text{Fr} = \frac{U}{Nh},$$

from the data; U is the wind speed averaged over the 1000-, 925-, and 850-hPa levels; N is the Brunt–Väisälä frequency calculated from the temperature difference between 1000 and 850 hPa; and the characteristic height h is found from the local orography. Also, we have calculated the component of the flow normal to the terrain,

$$V_t = \mathbf{V} \cdot \nabla Z,$$

where Z is the terrain height; positive values indicate upslope flow. When multiplied by the specific humidity q, this yields the moisture flux associated with flow normal to the terrain.

Finally, we have used a mesoscale numerical simulation model to assist with our diagnosis. The basic aspects of the model are described in detail in Nickerson et al. (1986); the version we used was the same as used in Romero et al. (1997), which is a modification of the version used in Ramis and Romero (1995). It is a hydrostatic, primitive equation nested-grid model, with a terrain-following vertical coordinate. Grid spacing in the model is 20 km in the horizontal and uses 30 levels in

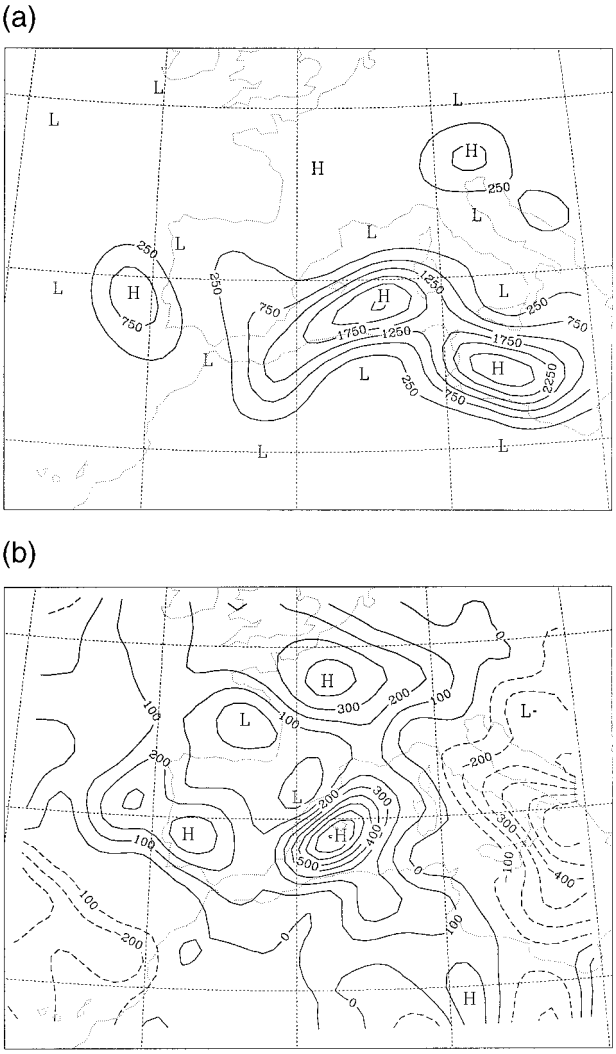

FIG. 9. Spatial distribution of (a) CAPE and (b) SRH at 1200 UTC 8 October 1992. The isopleth interval for CAPE is 500 J kg^{-1} starting at 250 J kg^{-1}; for SRH, the interval is 100 m^2 s^{-2}.

the vertical, with enhanced resolution in the planetary boundary layer. Initial and lateral boundary conditions (the latter are variable in time) are provided from the ECMWF model grids. The model is initialized on the mesoscale model grid from the relatively coarse ECMWF gridpoint values via a successive-corrections objective analysis (Pedder 1993), and the analyzed fields are subjected to a mass wind balancing before being used in the model. Convection is parameterized using the scheme developed by Emanuel (1991); details of the other physical parameterizations can be found in the references.

3. Synoptic structures and diagnosis

By looking only at the midtroposphere and near the surface, it might be possible to assert that most heavy precipitation events in the Mediterranean have basically similar synoptic patterns. For example, García-Dana et al. (1982), Llasat (1987), and Ramis et al. (1994) present case studies for situations in the western Mediterranean region that are characterized at low levels by an anticyclone located in the center of the European continent and a low to the west or southwest of Spain. This pattern produces advection of warm, humid air somewhere over the western Mediterranean. At midtropospheric levels, a trough (sometimes a cutoff low) is observed approaching the western Mediterranean region from the west on the day of the event, while a ridge dominates the eastern part of the western Mediterranean.

Our three cases certainly share these superficially similar synoptic structures, at least on the days when heavy precipitation occurred. However, as we shall see, the differences among the situations are much more important than the similarities. An important part of our motivation for considering these particular three cases is derived from their selection as ANOMALIA cases rather than any perceived synoptic similarities.

a. ''Menorca'' case

This case occurred on 7–9 October 1992 and produced heavy precipitation over the Valencia region of mainland Spain and over the Balearic Isles. Somewhat atypical, however, is the occurrence of a significant tornado[3] on Menorca (one of the Balearic Islands) at about 2000 UTC on 8 October. The 24-h precipitation collected during 8 October in the Valencia and Murcia regions, as well as the Balearic Isles, is shown in Fig. 4. We call this the ''Menorca'' case among the ANOMALIA events for rather obvious reasons.

As can be seen in Fig. 5a, the situation at 1200 UTC 8 October is characterized near the surface by low pressure to the southwest of the Iberian Peninsula, as well as a low over the southern portion of the western Mediterranean Sea. Warm thermal advection over the sea is very strong at 850 hPa (Fig. 5b) in the vicinity of the Balearic Isles. At mid- (500 hPa; Fig. 5c) and upper- (300 hPa; Fig. 5d) tropospheric levels, a dominant cyclone is located near the coast of Portugal, with a notable shortwave trough embedded in the circulation extending from the cyclone into northern Africa.

Convection develops initially in the southern portions of the western Mediterranean Sea around 0500 UTC 8 October. Figure 6a shows two convective systems that develop simultaneously over the sea, one near Andalucia (the ''southern'' storm) and the other near Valencia (the ''northern'' storm). The southern storm moves to the northeast but the other remains nearly stationary (cf. Fig. 6a with Fig. 6b). This differential movement pro-

[3] The tornado was rated F2 on the Fujita scale according to M. Gayá (1996, personal communication) of the INM in Palma, who did the poststorm survey.

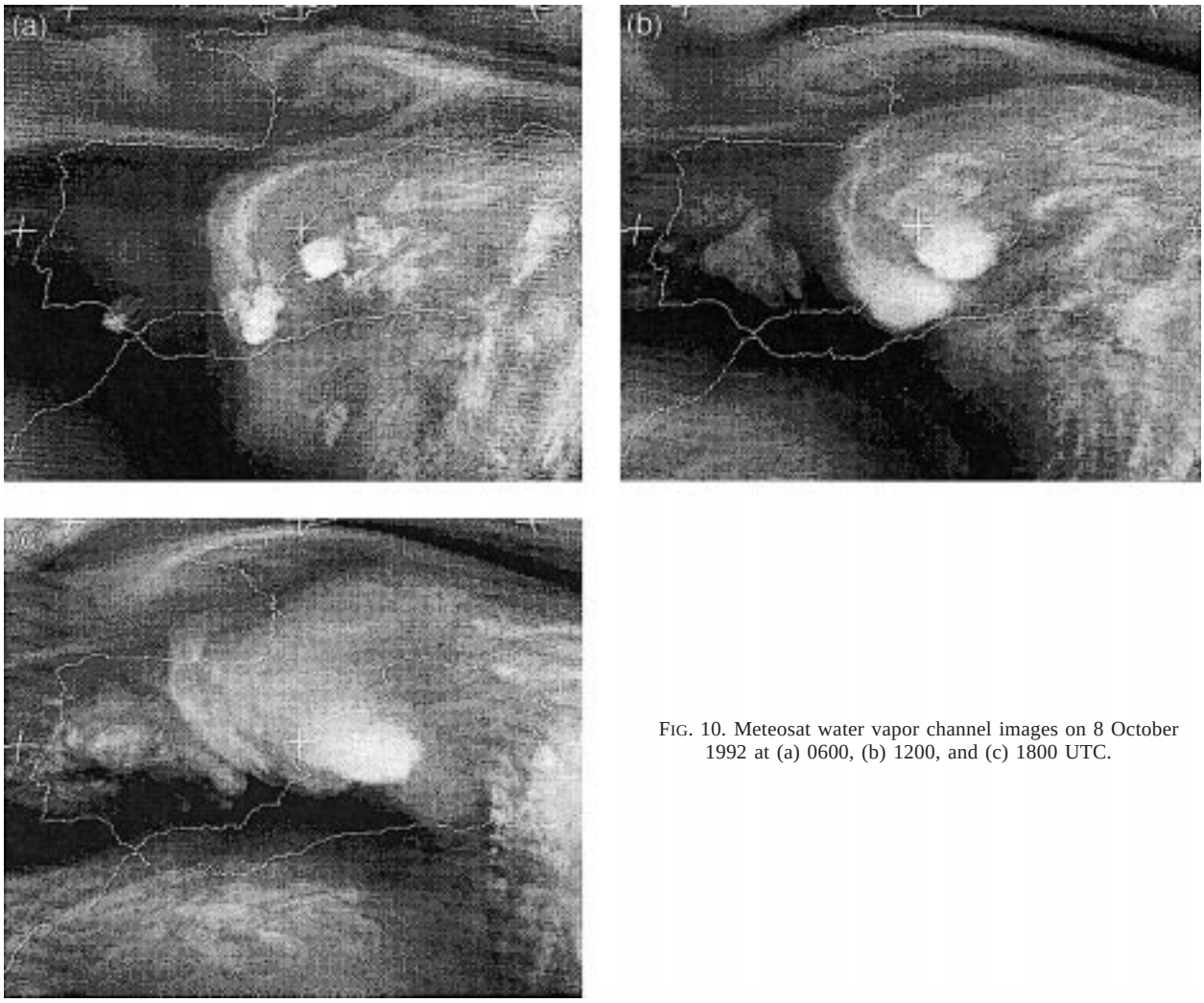

FIG. 10. Meteosat water vapor channel images on 8 October 1992 at (a) 0600, (b) 1200, and (c) 1800 UTC.

duces merger with the northern storm around 1400 UTC, as shown in Fig. 6c. The combined convective system moves to the northeast, passing over Menorca in the Balearic Islands when the tornado occurred, near the time of Fig. 6d. After the merger, the system is still ongoing as late as 0600 UTC 9 October (i.e., more than 24 h after initiation), on the French coast.

At low levels, quasigeostrophic forcing for upward motion (FQ) is relatively strong in the vicinity of the Balearics (Fig. 7a), but in the midtroposphere the highest values are to the southwest of the Iberian peninsula (Fig. 7b). The structure shown in Fig. 7a is consistent from 1000 through 700 hPa (not shown), although it weakens significantly at 700 hPa; the pattern changes substantially between 700 and 500 hPa. Since the convection develops over the Mediterranean Sea near the Balearics where the low-level FQ was favorable, the dominant contribution to FQ overall for the deep convection with this event is apparently associated with warm advection at low levels, like the cases shown by Maddox and Doswell (1982).

Water vapor flux divergence in the layer between 1000 and 850 hPa exhibits a convergent area from Andalucia to Catalonia, more or less covering the eastern Spanish coast, with the highest values over the sea close to the Valencia region (Fig. 8). Warm, humid air is over the sea to the southeast of the Balearic Islands, but CAPE is concentrated in the southern portion of the western Mediterranean (Fig. 9). The development of the convective systems takes place along the boundary of the region of most unstable stratification, where the CAPE distribution overlaps the low-level water vapor flux convergence region.

We have used the gridded data to estimate the soundings and hodographs in the vicinity of the two systems near their initiation time at about 0500 UTC. The southern storm developed where *ground-relative* helicity [equivalent to geostrophic thermal advection, as shown

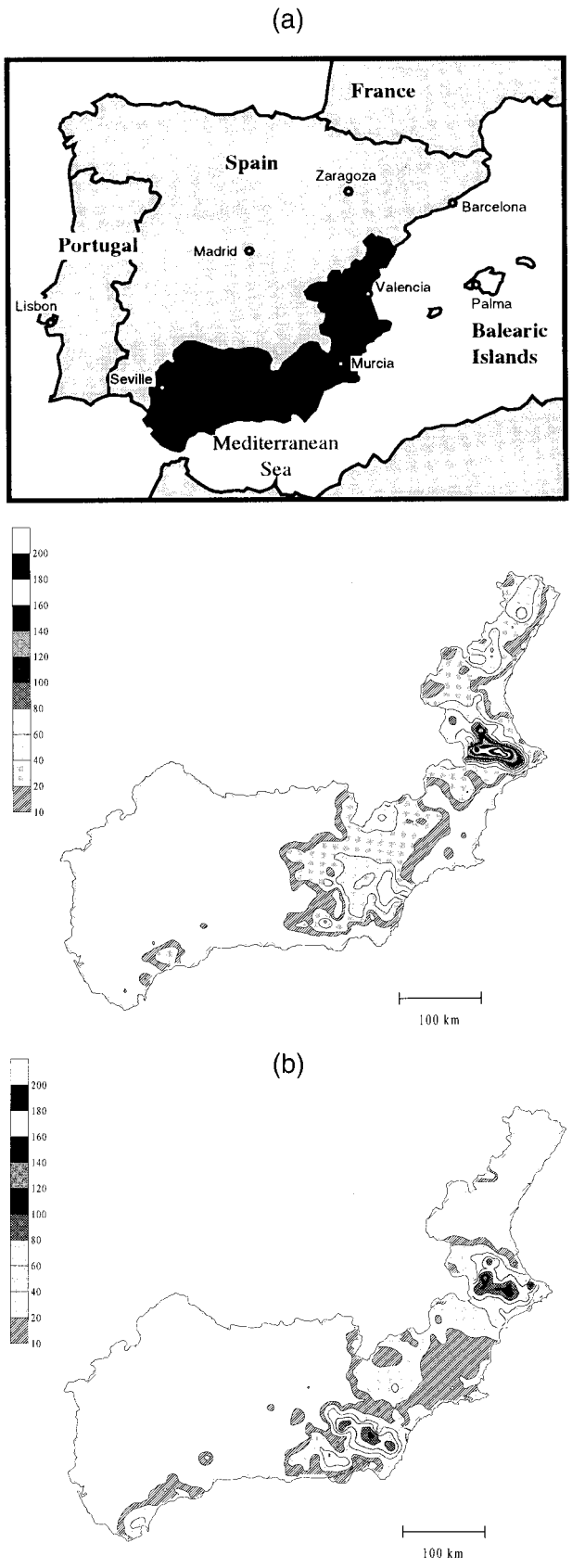

by Tudurí and Ramis (1997)] was higher than in the environment of the northern storm, and neither storm is apparently in a region of particularly high CAPE, according to the analysis. However, if we consider a sequence of water vapor channel Meteosat images (Fig. 10), it can be seen that a dry intrusion is associated with the development of the southern storm. The leading edge of the dry intrusion is roughly coincident with the shortwave trough shown earlier (cf. Fig. 5d). The trough remains linked with the southern storm and, later, with the convective system resulting from the ''merger'' of the two separate convective systems. Note also that the northern storm, the one producing the heavy precipitation, developed and remained in the moist air *ahead* of the dry intrusion prior to its merger with the southern storm.

The development of a tornado is evidence of the possible supercellular character of the convection, but not all tornadoes come from supercells. It is known that supercells develop in environments exhibiting at least some CAPE and SRH values on the order of 150 m^2 s^{-2} (Davies-Jones et al. 1990). We have investigated this possibility by using the spatial and temporal distribution of CAPE and SRH from the gridded data provided by the ECMWF. The storm motion used in finding the SRH (Fig. 9) is for the southern convective system, estimated to be from 220° at 17 m s^{-1}. This motion has been used since it is the motion that persists after the ''merger'' with the northern storm and hence is characteristic of the storm motion over an extended period. High SRH values can be seen in the vicinity of the Balearic Isles, in the vicinity of both convective systems. Although we have no data capable of giving an unambiguous confirmation that the storm was indeed a supercell, that hypothesis is at least consistent with the available data. The SRH distribution at the time of storm development (not shown) has peak values over the sea near where the southern storm developed. This SRH feature moves to the northeast, following the southern storm, and continues to follow the convective system after merger.

For this case, heavy precipitation [exceeding 100 mm (3.9 in)] is observed on the island of Ibiza (cf. Fig. 4) in the Balearics, although precipitation in Valencia does not quite reach 100 mm. Figure 6 shows that the quasi-stationary northern system remains mostly offshore throughout its evolution; Valencia may have only narrowly escaped a much more intense rainfall event. With easterly flow at low levels, perhaps enhanced by stable but moist outflow from the convective system, orographic enhancement of the rainfall (as noted in the Algeria case, the discussion of which follows) is a pos-

←

FIG. 11. Accumulated 24-h rainfall (mm) in Valencia, Murcia, and Andalucia regions (a) for the period 0700 UTC 1 February–0700 UTC 2 February 1993 (inset shows location of the area shown), and (b) for the period 0700 UTC 2 February–0700 UTC 3 February 1993.

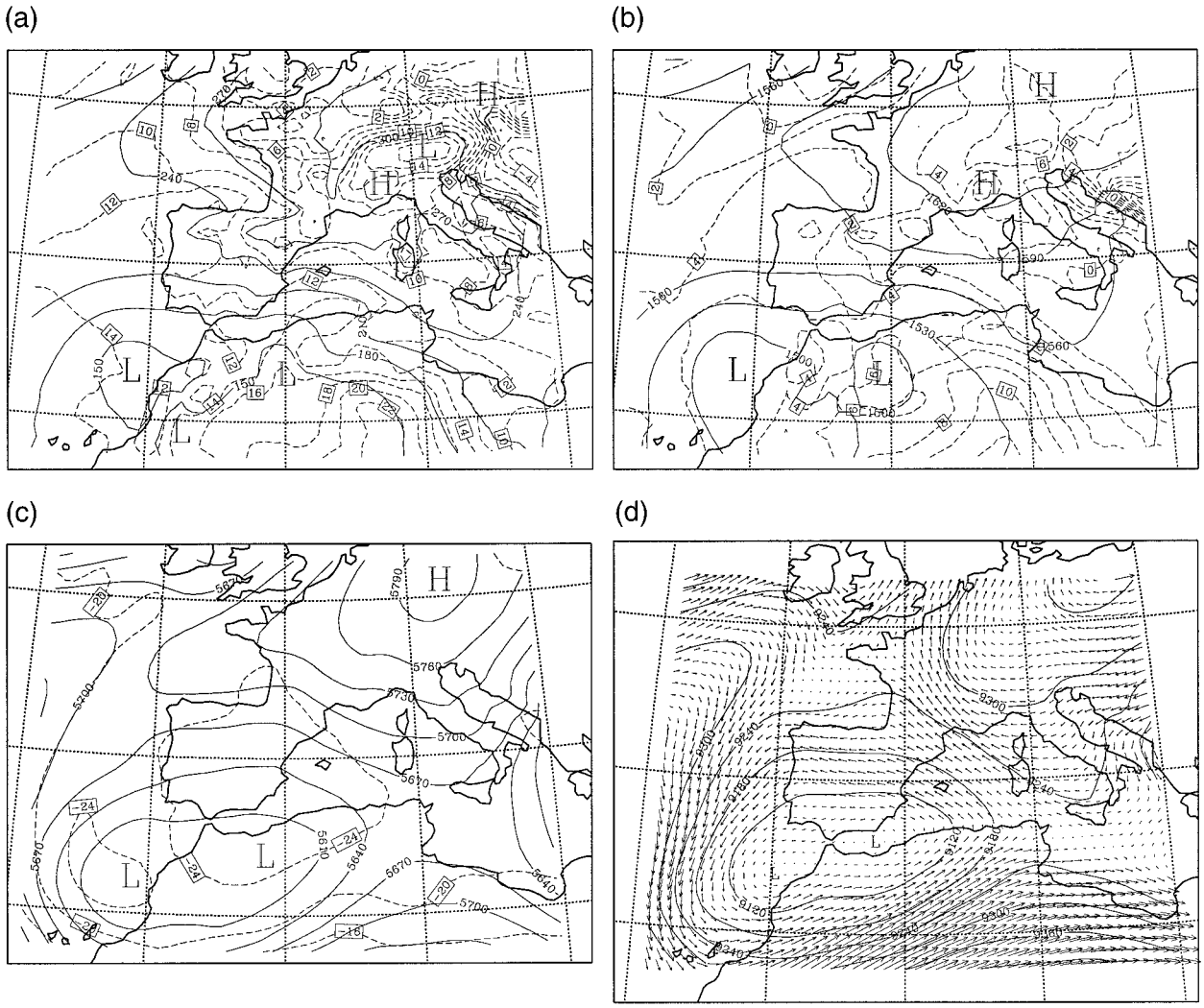

FIG. 12. As in Fig. 5 except for 0000 UTC 2 February 1993.

sible contributor to the moderately heavy rainfalls in Valencia. Given that the offshore air being lifted by the terrain in Valencia is only weakly unstable, it does not develop into deep convective cells (as observed) but might well produce significant rainfall when forced upward by orography [as in the Alaska case described by Doswell et al. (1996)].

On Ibiza, however, the heavy precipitation is associated with the quasistationary northern convective system, prior to its merger with the southern system. The Palma sounding (cf. Fig. 2) shows high humidity through most of the troposphere, indirect evidence for a high precipitation efficiency. By 1800 UTC, the combined convective system is over Mallorca, producing only moderate precipitation totals there. This system goes on to produce the tornado about 2 h later over western Menorca, accompanied by relatively light precipitation (about 10-mm maximum values recorded). The tornadic storm's minimal precipitation could have been associated with the intrusion of dry air aloft (as discussed above), which can alter a storm's precipitation efficiency. The storm also moves through Menorca relatively rapidly, limiting its precipitation potential by reducing the duration of the rainfall. Occasionally, supercells pose a heavy precipitation threat (see Doswell 1994), but the Menorca tornadic storm does not appear to be such a case.

b. ''Algeria'' case

Although this event also occurs downstream of a midtropospheric trough, the synoptic situation is quite different from the previous one. Precipitation occurs over an extended period (31 January–6 February 1993) during this case, with particularly heavy 24-h rainfall totals on 1 February in Valencia and Andalucia and on 2 February in Valencia. Figure 11 shows the amounts and

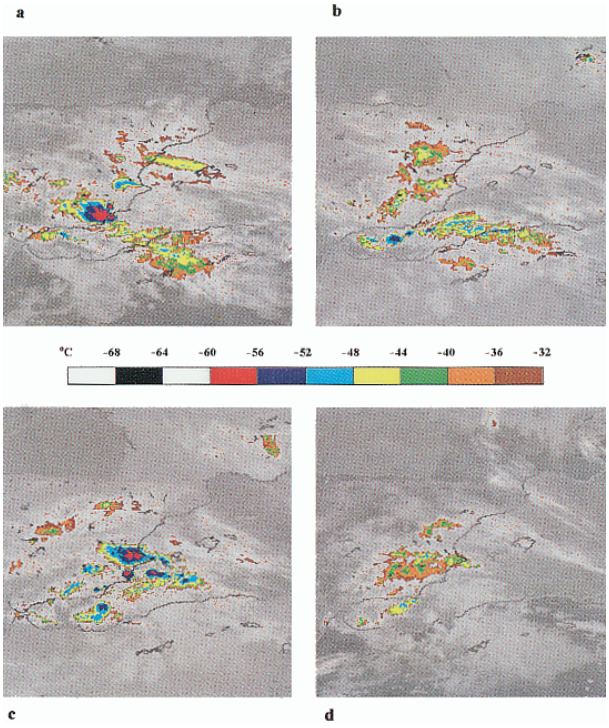

FIG. 13. Meteosat IR images at (a) 1200 UTC 1 February 1993 (b) 2000 UTC 1 February 1993, (c) 0400 UTC 2 February 1993, and (d) 1200 UTC 2 February 1993.

distribution of rainfall for the indicated regions and days.

This situation is somewhat unusual in that it occurred during the heart of winter, whereas most heavy rainfalls in the region happen during the months of October and November (Font 1983). The synoptic situation was basically stagnant during the period, with embedded mesoscale structures that controlled the timing and location of the heavy precipitation, as we will show in the next section.

Figure 12 shows the basic synoptic situation at 0000 UTC 2 February 1993. A low-level cyclone can be seen (Fig. 12a) in Algeria through much of the period. This low-level cyclone plays an important role in the event; thus, our name for the case. Whereas the midtropospheric cyclone of relevance for the Menorca case was moving, the large-scale structure remains almost stationary throughout the period in this case, with the apparent center of circulation located south of the Iberian peninsula. The slow movement is associated with substantially diminished low-level thermal advection in this case, in comparison to the Menorca case.

The mid- and upper-tropospheric views of the cyclone exhibit a double structure (Figs. 12c,d). Unfortunately, the diagnosis of subsynoptic-scale features is not completely reliable; these data simply are too coarse and the systems are located in data-sparse regions where it is not possible to be confident of the analysis (see Doswell and Caracena 1988). Subsynoptic features can be seen in animated loops of satellite images, but the quantitative aspects of such structures are too uncertain to be used in this overview.

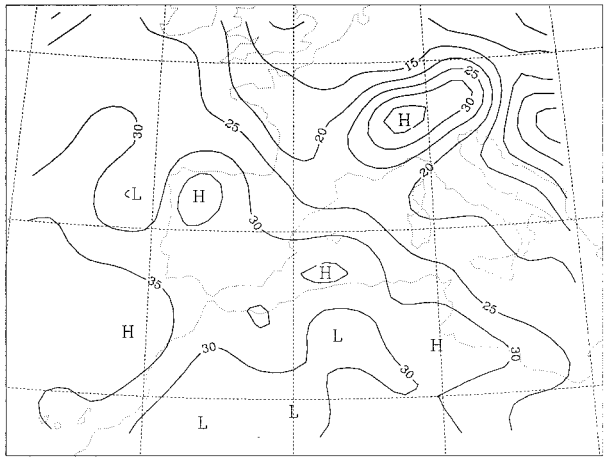

FIG. 14. Spatial distribution of θ_e (°C) at 1000-hPa surface at 0000 UTC 2 February 1993.

The satellite image sequence of Fig. 13 is representative of the event producing the precipitation observed for 1 and 2 February. Note that precipitation totals from the cooperative observations used in our rainfall analyses (Fig. 11) are valid from 0700 UTC on one day to 0700 UTC the next. Hence, the totals for ''1 February'' include any amounts falling between 0000 and 0700 UTC on 2 February. As can be observed in Fig. 13, it appears that considerable convection develops in the Valencia region before the 0700 UTC reporting time and continues well beyond that time. This is unfortunate, since at least some of the precipitation total for 2 February in Valencia probably includes a continuation of the rainfall that produced the large values on 1 February. Because virtually all of the rainfall observations are 24-

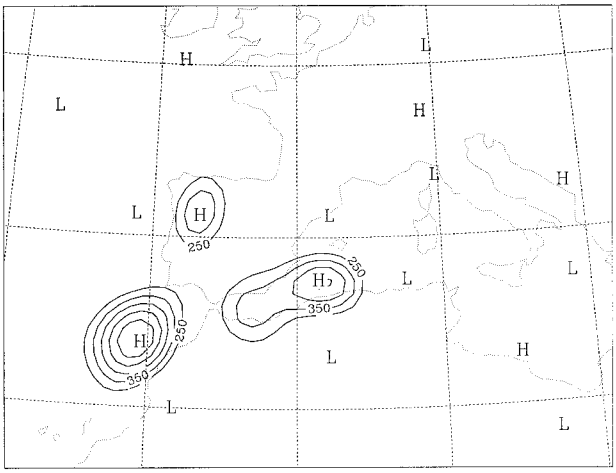

FIG. 15. Spatial distribution of CAPE at 0000 UTC 2 February 1993; isopleth interval is 100 J kg^{-1}, starting at 250 J kg^{-1}.

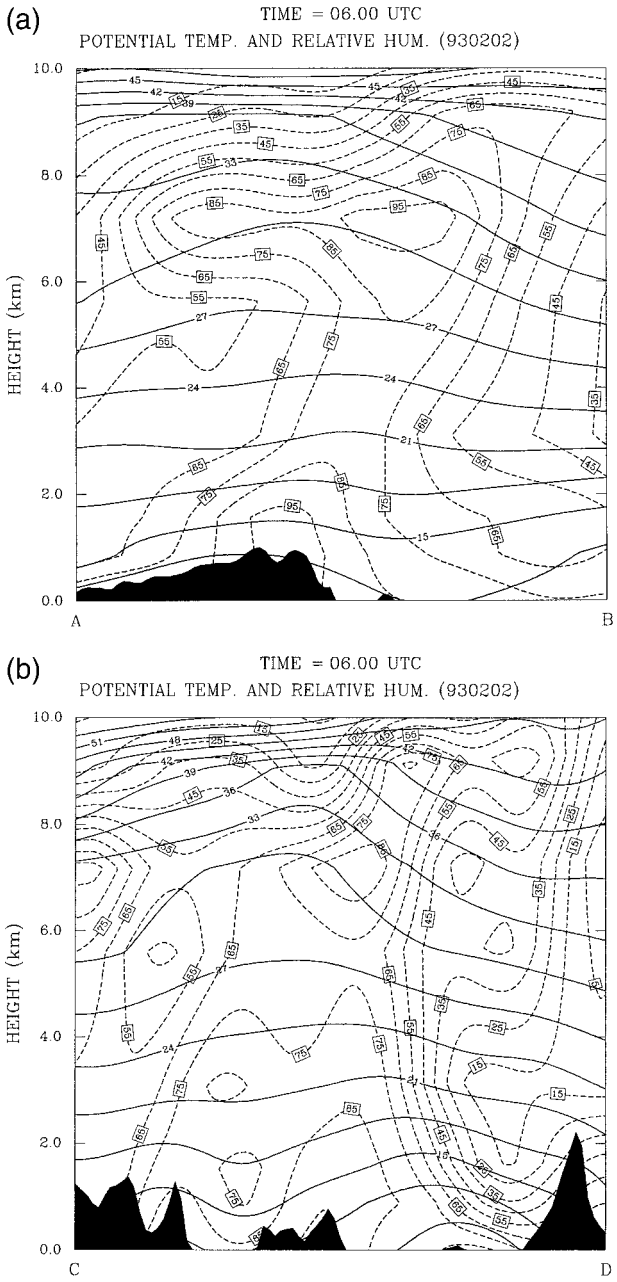

FIG. 16. (a) Cross sections at 0600 UTC 2 February 1993: (a) along the line AB and (b) along the line CD indicated in Fig. 1. Solid lines represent potential temperature (°C) and dashed lines represent relative humidity (percent).

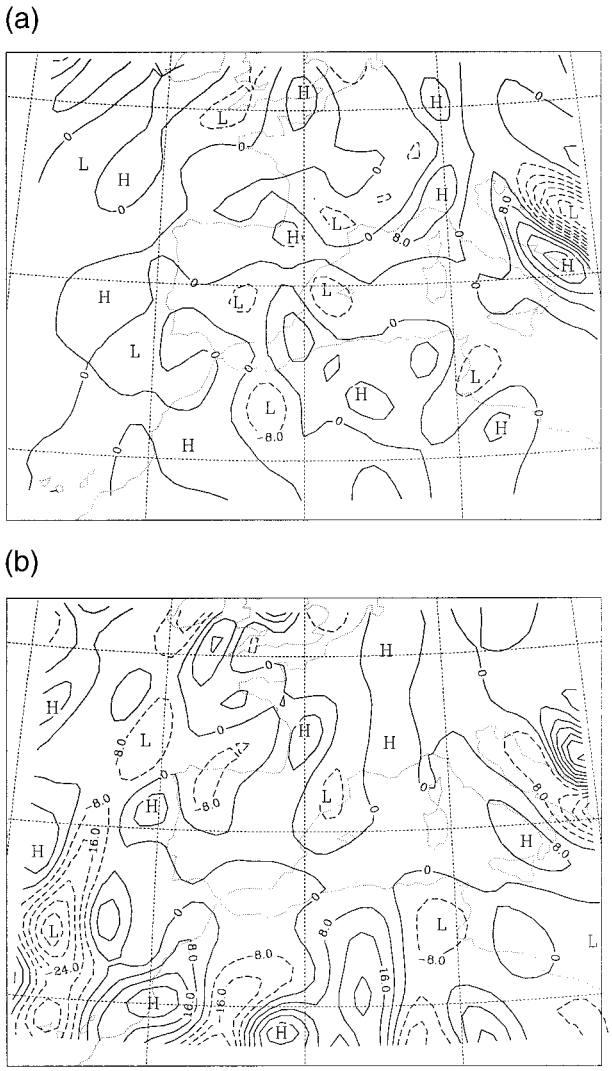

FIG. 17. As in Fig. 7 except for 0000 UTC 2 February 1993.

h totals and because there is no available archive of radar data that could be used to estimate rainfall, there is no simple practical solution to this problem.

Figure 13a also reveals that the precipitation in Andalucia is associated with a substantial convective system along a line of enhanced cloudiness that may be a reflection of a subsynoptic-scale trough oriented roughly northwest–southeast. Note the small cloud feature in Valencia at this time; it is unclear from available data how much (if any) precipitation occurs with this feature. Animated satellite image loops suggest it is anvil debris from a series of small, warm-topped convective clouds forming offshore. The cloud line seen with the Andalucia convection is moving northward and may play a role in the development of the convection seen in Figs. 13c,d that produces the heavy rains in Valencia.

Convective development occurs near the axis of *maximum* θ_e at low levels (Fig. 14), unlike the Menorca case where convection developed on the *boundary* of the high θ_e air. There is not much CAPE available (Fig. 15) along the θ_e boundary; instead, what modest CAPE[4] that exists is associated with the highest θ_e available.

A feature of considerable interest during this episode

[4] Note that CAPE of 250 J kg^{-1} supports a pure parcel theory maximum updraft exceeding 20 m s^{-1}.

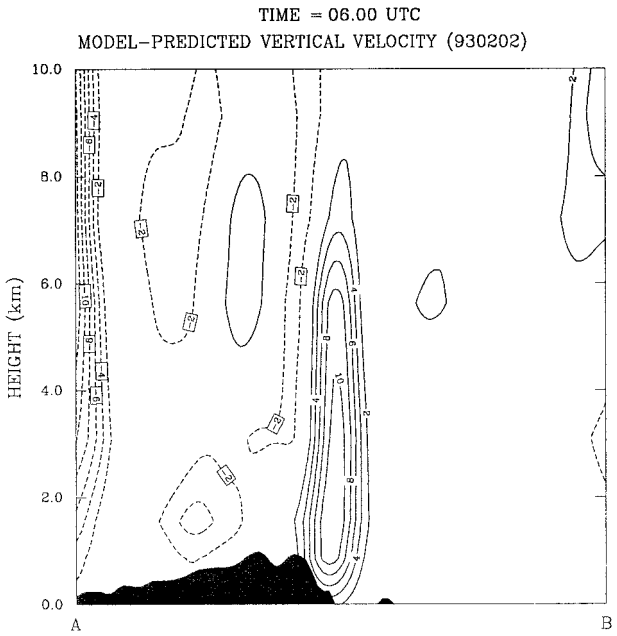

FIG. 18. Cross section along AB (see Fig. 1) of model predicted vertical velocity at 0600 UTC 2 February 1993; the isopleth interval is 2 cm s^{-1} and solid lines indicate upward motion. The distance AB is 1800 km, so the width of the ''plume'' is about 150–200 km.

is revealed by two cross sections (the locations of which are indicated in Fig. 1). Along the eastern coast of mainland Spain, a deep vertical column of enhanced relative humidity with relatively dry air on either side persists for days along cross section AB (Fig. 16a). The potential

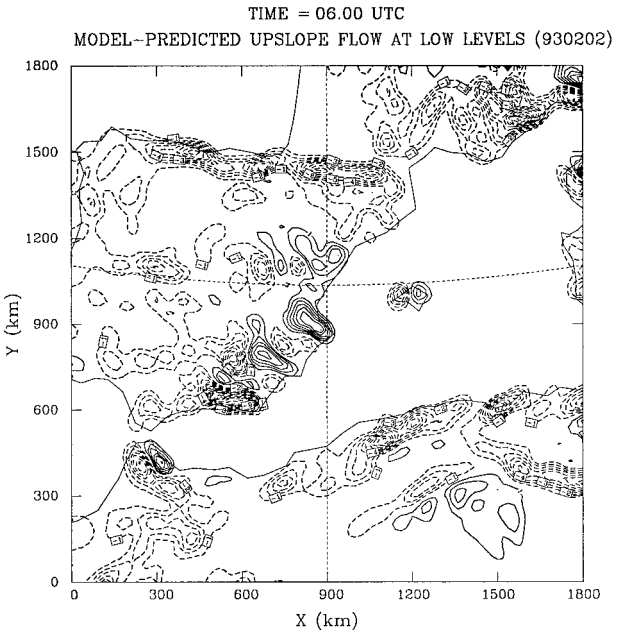

FIG. 19. Model-predicted upslope flow at the lowest atmospheric level corresponding to 0600 UTC 2 February 1993; the isopleth interval is 1 cm s^{-1} and solid lines indicate upward motion.

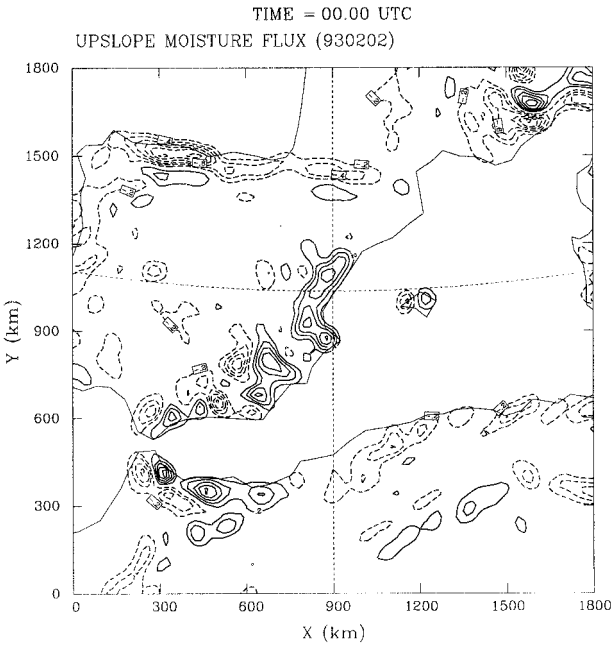

FIG. 20. Upslope moisture flux, qV_U, at 0000 UTC 2 February 1993; isopleth interval 0.2 g kg^{-1} cm s^{-1}, starting at 0.2 g kg^{-1} cm s^{-1}.

temperature distribution reveals by the spacing between isentropes that the plume is also in a region of low static stability. Along CD (Fig. 16b), it can be seen that this plume is concentrated along the southeastern Spanish coast, roughly corresponding to the region receiving the heavy rainfalls through the period 1–3 February. During this period, there is a tendency for the features of interest to move slowly north-northeastward, such that at the end of the episode, the precipitation is mainly in northern Valencia and Catalonia.

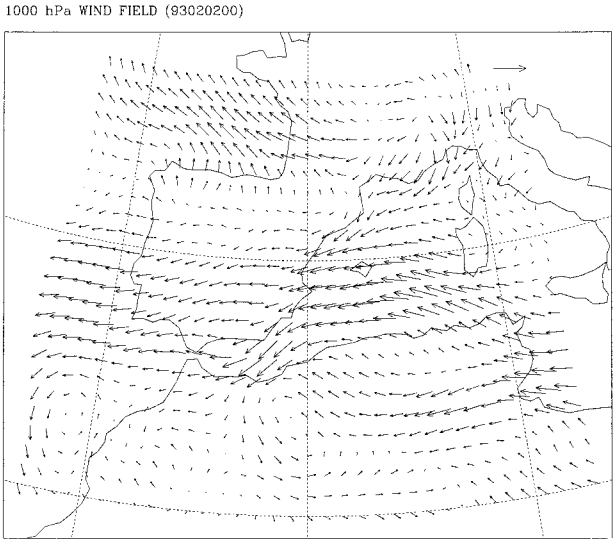

FIG. 21. Wind field at 1000 hPa at 0000 UTC 2 February 1993 from ECMWF data. The arrow in the upper-right corner represents 20 m s^{-1}.

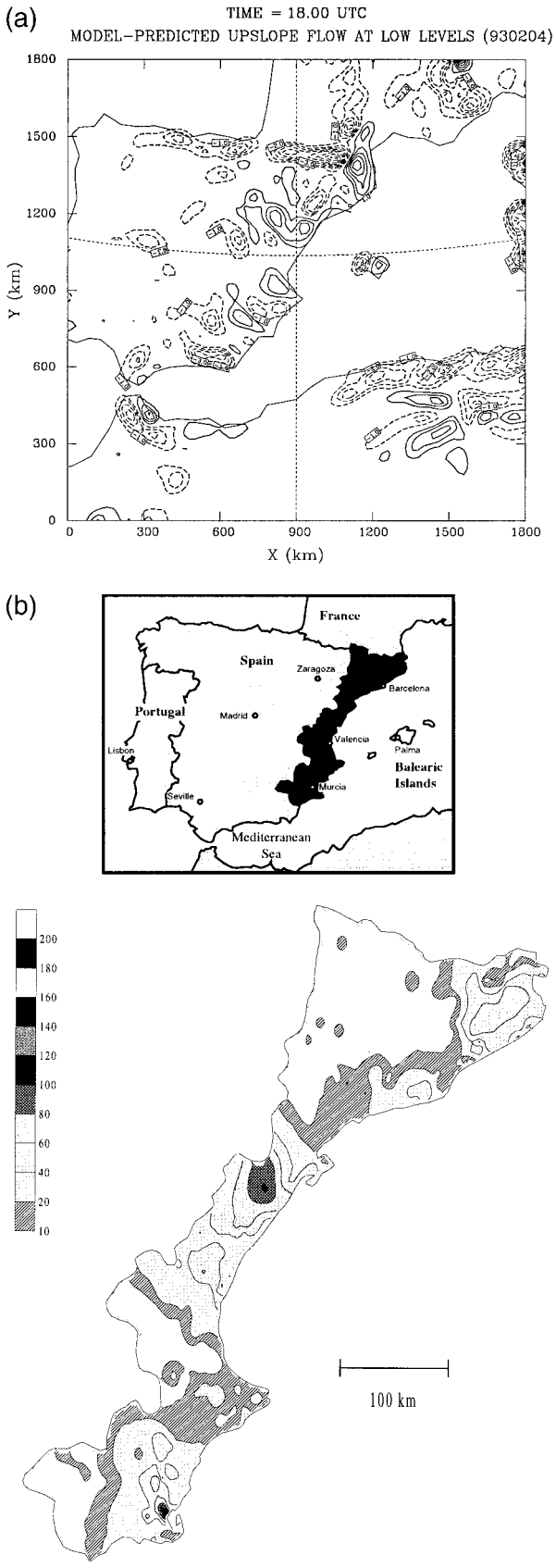

The FQ for this event, shown in Fig. 17, does not exhibit any obvious correlation to this persistent plume of high humidity along the coast of Spain. Overall, the nearly equivalent barotropic structure of the atmosphere in middle levels provides little clear signal for large-scale FQ. It is difficult to associate the plume of high humidity with any features in the FQ field. What are its origins?

Since we did mesoscale numerical model simulations of all our cases [results of the simulations are discussed in Romero et al. (1998), hereafter RRADS], the model forecasts have turned out to be helpful for understanding this event. Figure 18 reveals that the numerical simulation produced a ''plume'' of deep upward vertical motion that approximately coincides with the observed plume of high relative humidity (cf. Fig. 16). The simulation seems to have captured many of the details of the low-level flow (not shown), and it appears that the plume is a reflection of sustained upward motion induced by the interaction between the low-level flow and the orography. This concept is validated when we compare Figs. 19 and 20 with Fig. 11, showing a reasonably good comparison between the model-simulated upslope flow and the observed upslope moisture flux at low levels with the observed precipitation. Since the model's upward vertical motion peak is well above the terrain, this suggests both a convective and an orographic component in that vertical motion. The Froude number calculation yields Fr = 1.81, indicating vigorous ascent is possible and, presumably, enough lift to initiate buoyant convection.

Flow fields at low levels are what one would expect in this overall synoptic pattern, with easterlies impinging on the coast of Spain, enhanced by the presence of the ''Algerian'' low-level cyclone (Fig. 21). Minor day-to-day variations in the flow occur through the period. It is known that orographically induced cyclones of the sort seen at low levels in this case are important in rainfall events of the region (e.g., Romero et al. 1997; Ramis et al. 1994) and that the rainfall in Valencia is strongly sensitive to the low-level flow direction Valencia (R. Armengot 1997, personal communication). It has been observed by forecasters there that slight variations in the flow at low levels can shift the focus of orographically created rainfall to a different location or can prevent it entirely (Fig. 22).

The day-to-day patterns of instability (not shown) reveal a slow increase in the CAPE values leading up to the heavy rainfalls, as well as an increase in the areal extent of the positive CAPE through the first half of the period. Figure 23 shows that this is clearly associated

←

FIG. 22. (a) As in Fig. 19 except at 1800 UTC 4 February 1993. (b) Accumulated 24-h rainfall (mm) in Valencia, Murcia, and Catalonia regions (inset shows locations) for the period from 0700 UTC 4 February to 0700 UTC 5 February 1993.

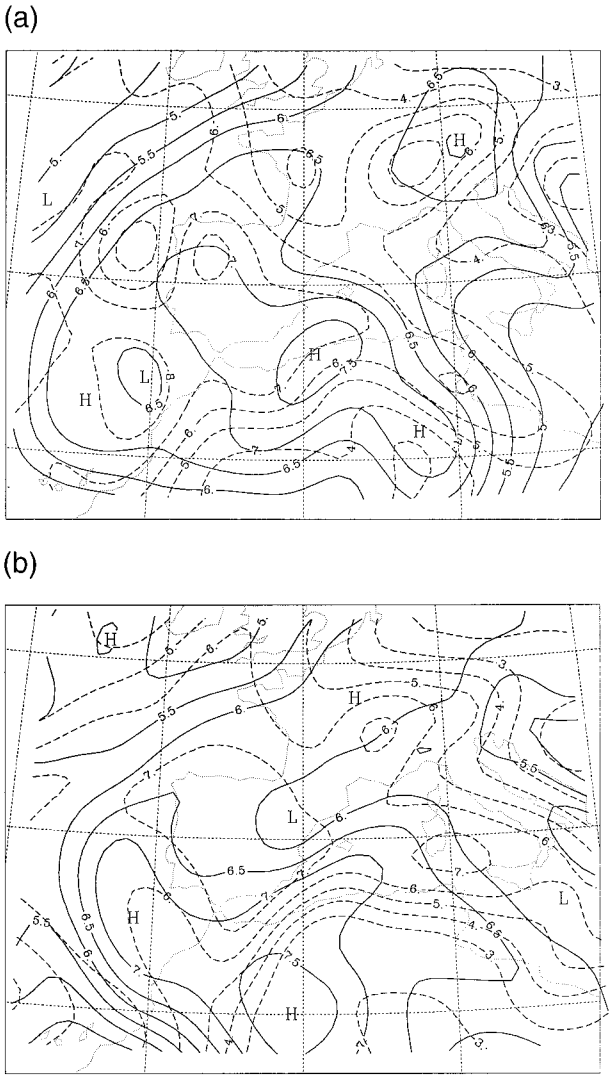

FIG. 23. Lapse rate (solid line) between 850 and 500 hPa and mixing ratio (dashed line) at 1000 hPa at (a) 0000 UTC 2 February 1993 and (b) 0000 UTC 3 February 1993; isopleth interval for lapse rate is 0.5 K km^{-1}; for mixing ratio 1 g kg^{-1}.

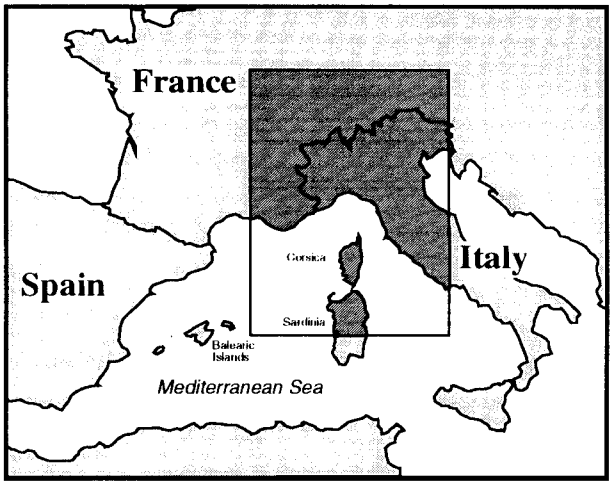

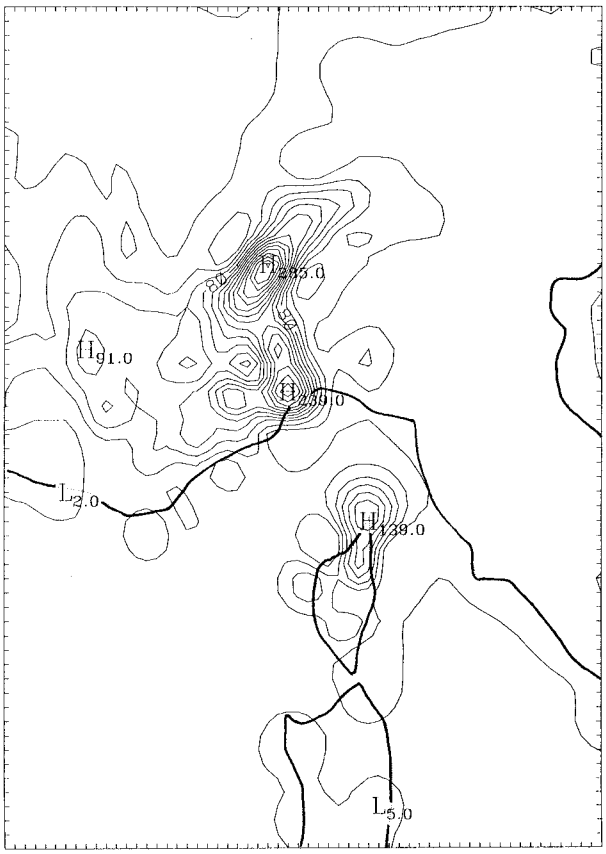

FIG. 24. Accumulated 24-h rainfall in mm, for the period from 0000 UTC 5 November to 0000 UTC 6 November 1994 in the Piedmont region and southeastern France (inset shows location).

with a superposition of slowly increasing low-level moisture with regions of increasing lower midtropospheric lapse rates (cf. Fig. 15).

Although the synoptic pattern in this case indicates that the likelihood of precipitation is relatively high throughout the period, it is difficult to *localize* regions of greatest threat in space and time. Much of the region ahead of the nearly stationary synoptic cyclone is characterized by weak quasigeostrophic forcing for upward motion, so the day-to-day changes in the location of the significant rainfalls do not seem to be related very clearly to synoptic-scale processes. To some unknown extent, the combination of the nearby modest FQ favoring upward motion (cf. Fig. 17a) and the favorable low-level moisture flow may have been sufficient to draw attention to Valencia. However, the excessive rainfall was quite confined in geographical extent, and synoptic-scale concepts are not sufficient to anticipate these details.

The stagnant synoptic situation also allowed an initially dry and stable cool season air mass to be transformed into one with modest CAPE, capable of sup-

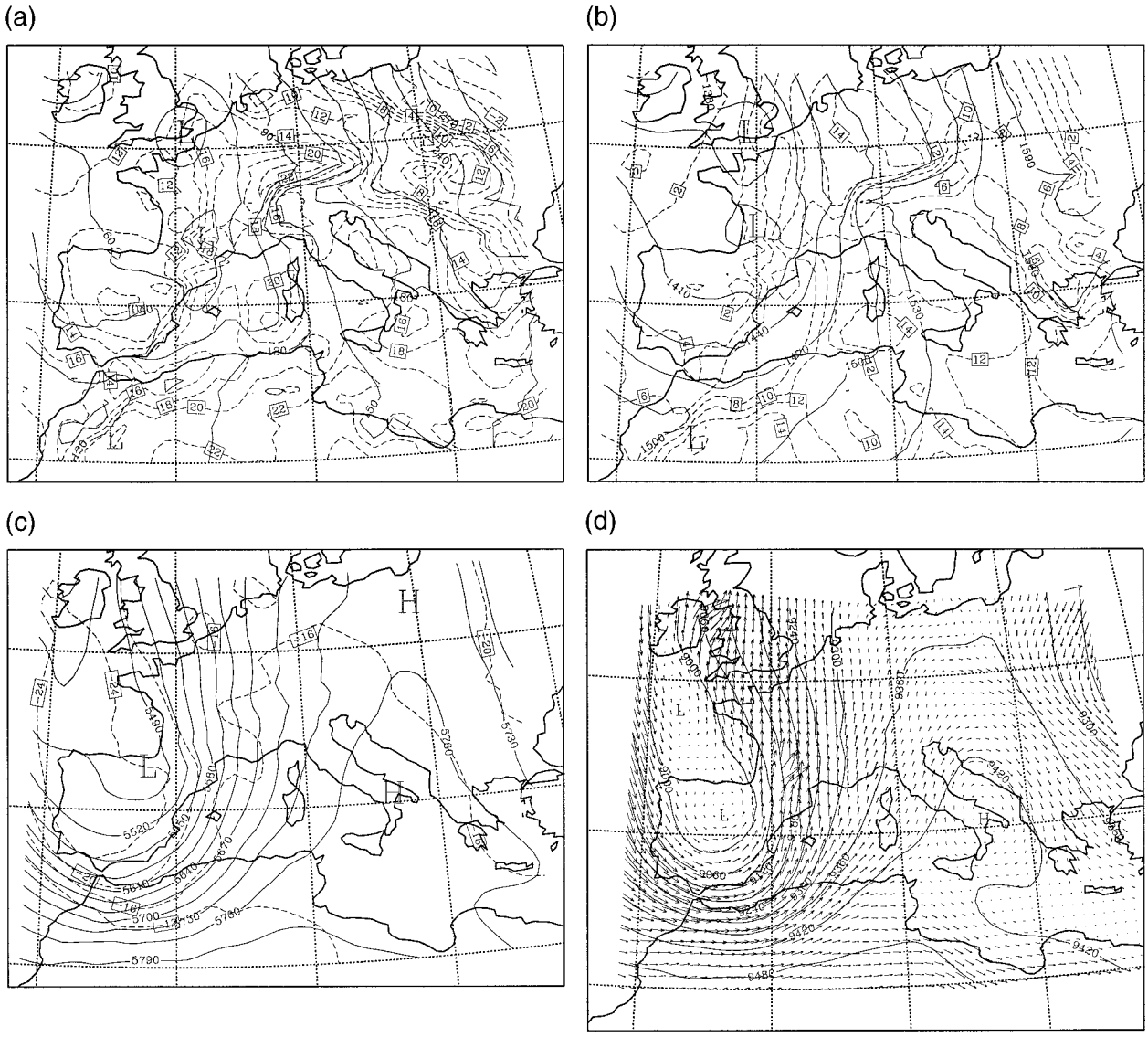

FIG. 25. As in Fig. 5 except for 0000 UTC 5 November 1994.

porting a few isolated heavy convective cells at an unusual time of the year for such events. The continued long fetch of easterly flow over a relatively warm ocean moistened the low-level air during its passage over the water and it was this moisture that produced the heavy precipitation (this hypothesis is considered in more detail in RRADS). However, precisely where and when the precipitation would fall seems to have depended sensitively on the interaction of that low-level flow with the terrain. Each day's heavy rain potential was high *somewhere* along the eastern Spanish coast during this persistent synoptic situation, but it appears that a very precise and accurate forecast of the low-level flow would have been necessary to obtain an accurate forecast of the specific location(s) of each day's heavy rainfall.

c. "Piedmont" case

This third event is quite interesting, because an important part of the rainfall appears to be predominantly nonconvective. Although rainfall was not limited to northwestern Italy, the majority of damage and casualties [6400 billion lira[5] and about 65 deaths, according to Lionetti (1996)] occurred there, in what is known as the Piedmont region (Fig. 1). Hence, our name for the case comes from this region. Maximum daily rainfall amounts on 5 November 1994 (Fig. 24) exceed 200 mm (7.9 in.) in the northwestern portion of the area, close

[5] At the approximate exchange rate, this figure corresponds to about $4 billion (U.S.).

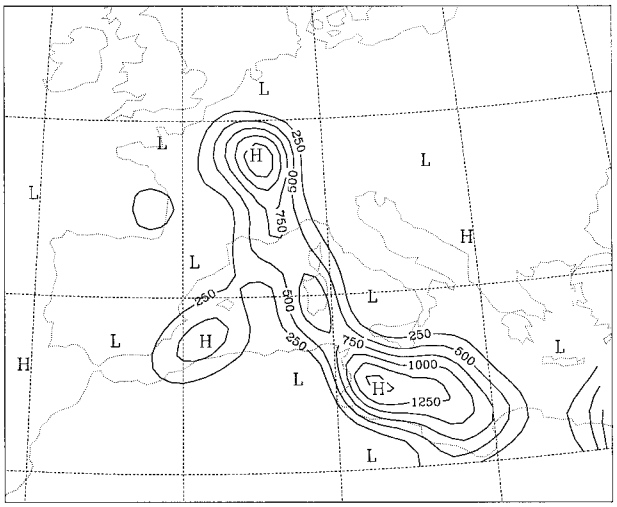

FIG. 26. Spatial distribution of CAPE at 1200 UTC 5 November 1994; isopleth interval is 250 J kg^{-1}, starting at 250 J kg^{-1}.

to the Alps. Another maximum in observed precipitation can be seen near the Italian coast. The spatial extent of the significant precipitation is much larger in this case than in the previous ones.

As with the other cases, a midtropospheric, synoptic-scale trough is present (Fig. 25) upstream from the precipitation area. This trough is also a mobile one like the Menorca case, not stagnant, as with the Algeria case. A cold front can be seen clearly at 850 hPa just to the east of Balearic Isles at 0000 UTC 5 November. This front is the western boundary of a region of moderate CAPE (Fig. 26) at 1200 UTC 5 November, but the region of instability is primarily over Italy and the Mediterranean Sea westward from Sardinia to the Balearic Isles, with another maximum in central France.

The evolution of the synoptic situation is illustrated by the changes over 24 h from 0000 UTC 5 November to 0000 UTC 6 November (Fig. 27). Frontal movement is relatively slow, such that by 0000 UTC 6 November, the front is just east of the islands of Sardinia and Corsica (Fig. 27b). During this period, a strong jet streak moves through the base of the trough and the trough overall is lifting out to the east-northeast. The zone of synoptic-scale forcing in the middle and upper troposphere (Figs. 27 and 28) is well upstream of the Piedmont region during the day of 5 November, still only approaching the coastline by 0000 UTC 6 November, at which time the heavy rainfalls are essentially over.

Rather than explosive convective developments over the Piedmont region, the satellite images (Fig. 29) indicate a large, indistinct cloud mass moving over northwestern Italy, connected to what are more obviously convective storms over the Italian coastline and extending over Corsica and Sardinia. A secondary convective band is still offshore by 0000 UTC 6 November. The low-level flow to the east of the boundary over Corsica and Sardinia is essentially southerly, providing a substantial upslope component over the foothills of the Alps in the Piedmont area (Fig. 30). Thus, it appears that much of the rainfall is associated with upslope flow of weakly stable, moist air. For this case, the Froude number is much lower (Fr = 0.90) than in the Algeria event, suggesting there might be some tendency for the upslope flow to be blocked by the terrain rather than going over it. However, for a saturated layer, the effective stability may be somewhat less than for unsaturated conditions; the satellite imagery showing considerable cloudiness (cf. Fig. 29) suggests a nearly saturated environment. The low-level moisture values in the moist air impinging on the Alps are significant, even if the CAPE is modest (recall Fig. 26). Hence, as in a case of heavy rainfall in the Kenai Peninsula of Alaska, presented in Doswell et al. (1996), the vertical motion associated with upslope flow appears to have been sufficient to produce significant rainfall in spite of the relative stability of the moist air.

The FQ fields (Fig 28) derived from the synoptic charts apparently are associated with the secondary convective band, rather than with the heavy rainfall. Instead, it seems that the rainfall inland is being generated by orographic ascent; only the coastal precipitation and that over Corsica appear convective. Heavy precipitation did not fall within a time span of a few hours, as is typical with a convective event. Rather, the rainfall persisted much of the day on 5 November, with average rates of perhaps 10–20 mm h^{-1} (Lionetti 1996),[6] also indicating the likelihood of a predominantly nonconvective nature for this event. The heavy rainfall along the Alpine slopes in the Piedmont region was forecast reasonably well by a mesoscale numerical simulation model (as discussed in RRADS), and the model's precipitation over the region was not associated with the model's convective parameterization. This adds credence to the conclusion that the precipitation on the Alpine slopes of the Piedmont region was not primarily convective in character.

4. Discussion and conclusions

This set of cases reveals a number of implications for the meteorology of heavy precipitation in the western Mediterranean region. Our diagnosis of the cases varies from one event to the other because each event had different aspects to be investigated. This underscores a need to use physically relevant diagnostic parameters. The all-important details associated with each case force the diagnostician to have access to a flexible set of diagnostic tools and to be able to recognize what tools are appropriate in any given situation. Our cases illustrate only some of the diagnostics that might be relevant

[6] Additional (unpublished) materials on this case documenting the precipitation can be found at the following World Wide Web site: http://www.map.ethz.ch/NL2.

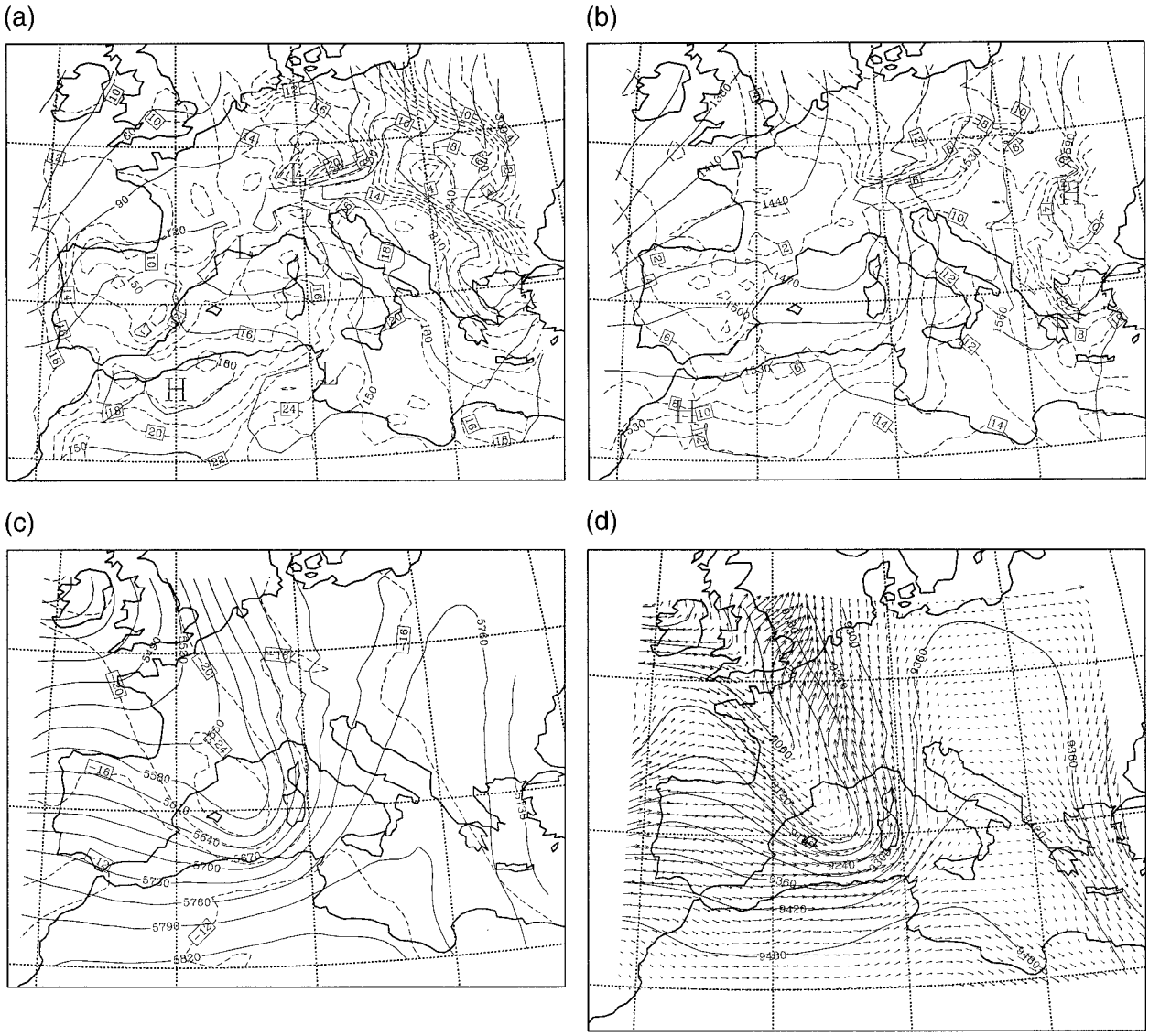

FIG. 27. As in Fig. 5 except for 0000 UTC 6 November 1994.

for a particular case (see Doswell et al. 1996 for further discussion).

Heavy precipitation in the western Mediterranean region usually occurs in the autumn, since the Mediterranean Sea surface temperatures are still high from the summer heating while the onset of autumn increases the chances for strong synoptic forcing. The structure of the Menorca case is quite complex and some aspects remain unexplained, even after the fact, given the data and the development of the convection over the data-poor oceans. Of our three ANOMALIA cases, it is the one most dominated by convection and, apparently, important but unobserved mesoscale details. The major feature associated with the event, the shortwave trough, is not clearly depicted in the conventional upper-air charts, a not-uncommon occurrence. Whereas the synoptic-scale diagnosis gives pretty clear indications of the potential for heavy precipitation and even reveals the possibility of supercells, the detailed evolution of the event, notably the quasistationary storm that develops over the sea to the east of Valencia, is not easily explained. Owing to the relative proximity of the two convective systems, the differences between the northern and the southern systems are a challenge to understand.

The Algeria case represents a different sort of challenge for forecasters. Since it is occurring at a time of the year when heavy precipitation events are climatologically rare, forecasters need to remember that being atypical is no protection against an event's occurrence. For this case, the stagnancy of the synoptic pattern is a key element; this permitted the destabilization of the low-level air mass over several days. Whereas Romero

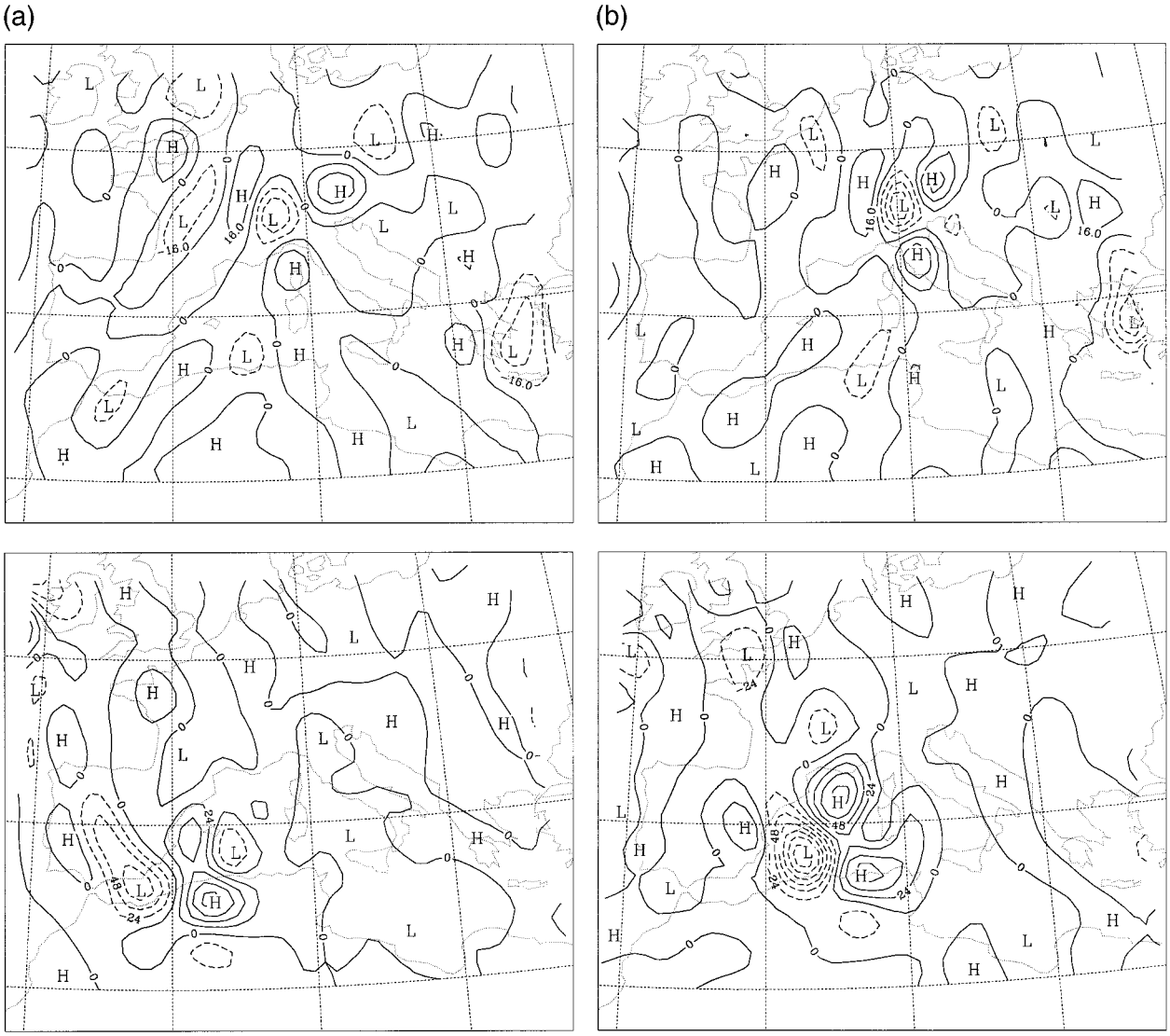

FIG. 28. As in Fig. 7 except for at (a) 1200 UTC 5 November 1994, and (b) 0000 UTC 6 November 1994. Isopleth intervals vary but are integer multiples of 8×10^{-18} m kg^{-1} s^{-1}.

et al. (1997) have shown that on any given day, surface fluxes of sensible and latent heat at times may not be important for that day's convective events, over a period of several days such fluxes can be very important in transforming the air mass. This airmass transformation, in turn, allowed the potential for heavy precipitation. However, the localization of the convection on each day appears to have been the result of subtle day-to-day shifts in the interaction between the low-level flow and the orography. Forecasting this might be quite difficult, and it is encouraging that the mesoscale numerical simulation experiments (RRADS) show some promise in providing guidance to forecasters.

Finally, the Piedmont case exemplifies a situation that forecasters in regions with complex terrain, like the western Mediterranean region, need to be able to anticipate: even nonconvective precipitation created by persistent terrain-induced forced ascent can be dangerously heavy. If ascent is via forced rather than buoyant ascent, the result still may be heavy precipitation. In this case, both types of processes were operating at the same time, but in different geographical regions. The absence of buoyant instability is no cause for complacency with respect to heavy precipitation.

Like their counterparts elsewhere in the world, convective storms in the western Mediterranean region respond to changes in their environment. The Menorca case, for example, suggests quite strongly that the dry intrusion was a factor in changing the character of the convection. Ahead of the dry air aloft, the storms were slow moving and apparently had high precipitation efficiency (which is promoted in moist environments like

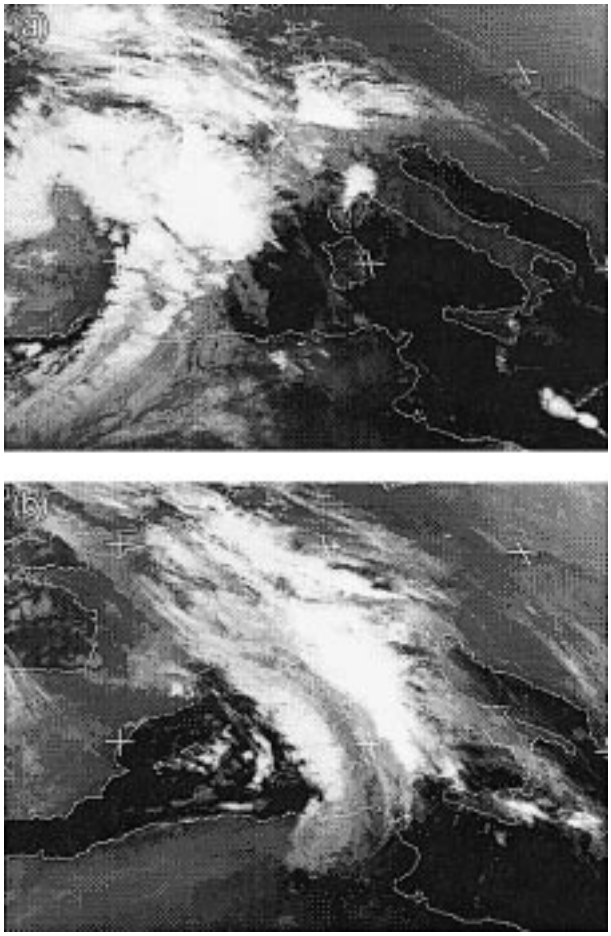

FIG. 29. Meteosat IR images for (a) 0000 UTC 5 November 1994 and (b) 0000 UTC 6 November 1994.

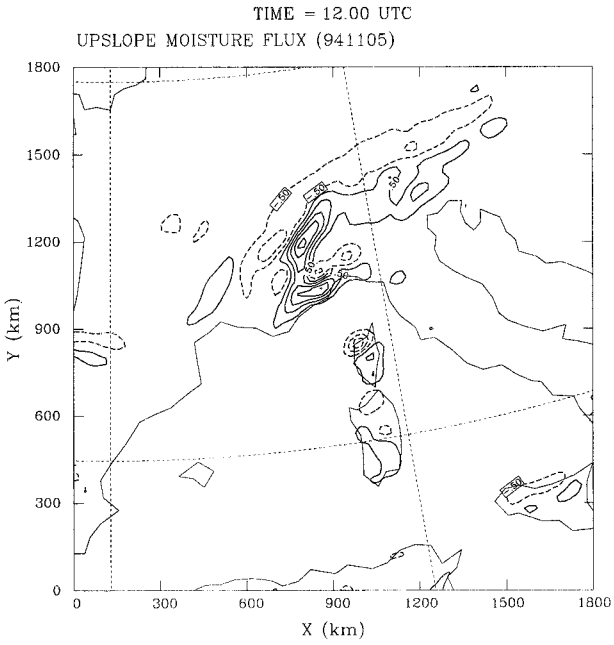

FIG. 30. As in Fig. 20 except for 1200 UTC 5 November 1994.

that shown in Fig. 2, and reduced in dry environments), judging by the observed rainfall amounts. In the vicinity of the dry intrusion, the convection did not produce heavy precipitation, but severe convective phenomena occurred.

The Mediterranean Sea itself and the complex terrain features surrounding it form a large topographic component in all three of these ANOMALIA cases. In some sense, the combination of strong synoptic-scale forcing and the importance of topographic features make the western Mediterranean region ideal for applications of mesoscale numerical simulations. When the orography induces mesoscale features (e.g., the ''Algerian'' cyclone to the lee of the Atlas Mountains) that play a role in an event, it is not only possible for a mesoscale model to anticipate such a development, but human forecasters should also be aware of that potential and should learn to account for it in their prognoses.

Heavy rainfall events are always difficult to forecast because of the inherently quantitative nature of the prediction. Predicting the *occurrence* of rain is easier than predicting the *amount* of rain in any specific location (Doswell et al. 1996). Nevertheless, it is expected of forecasters that they should be able to provide useful information about the potential for hazardous rainfall events. Although virtually all documented heavy precipitation episodes in the region arise ahead of midtropospheric troughs (e.g., Llasat 1987; Ramis et al. 1994), our study indicates that important structural and evolutionary differences exist among these events. Forecasters must take the task of diagnosis seriously if they are to have much hope of anticipating events.

Although we have presented a case (the Piedmont event) where some of the heavy rainfall occurred nonconvectively, such a situation is not really representative of most hazardous rainfalls in the western Mediterranean.[7] Convection plays an important role in most such events in the region, so forecasting the occurrence of deep convection is a critical part of any precipitation forecast. Because of this, it can be useful to try to anticipate the development of CAPE prior to its actual appearance on a diagnostic chart by following the progression of moisture and lapse rate separately. Moreover, by monitoring low-level moisture separately, the potential for nonconvective heavy rainfall can be assessed. Even when the ascent is orographically forced, there still is a need for substantial moisture content in the rising air.

In the Algeria case, it is noteworthy that the satellite signatures associated with the case are much less impressive for the early convection in Valencia than for

[7] Nonconvective heavy rain occurs in other parts of the world (e.g., the west coast of the United States, New Zealand, etc.).

the convection farther south. What is most relevant about the convection that produces heavy rain is its *persistence*, not its top height or the size of its cold anvil (see Doswell et al. 1996). For this case, the early convection on 1 February may not have produced the heaviest rainfall, but antecedent precipitation often is a factor in flash flood cases. This is by no means a new observation, but it is worth repeating: dangerous and important convective storms are not always the ones with the highest tops and the largest anvils. Just because a convective storm is small and has a warmer top is no reason to disregard it.

Clearly, three cases are not sufficient to make overly broad generalizations. We hope eventually to be able to develop a synoptic climatology of heavy precipitation in the region, based on a much larger set of cases than we have considered here. We want to know the frequency with which heavy precipitation episodes match the broad synoptic pattern that we have seen is common to all three of our cases (and others documented in the literature). A synoptic climatology might reveal other ''recipes'' for heavy precipitation than the three cases we have described, thereby indicating other diagnostic tools that might be needed.

Acknowledgments. This work was partially supported by EC under Grant EV5V-CT94-0442. The lead author was visiting the UIB under Grant DGICYT SAB95-0136. Meteosat images were generously provided by Prof. J. L. Casanovas of the University of Valladolid. Dr. V. Levizzani (FISBAT, Bologna, Italy) is acknowledged for his help with satellite image interpretation. Precipitation data were provided by INM of Spain and by Dr. A. Buzzi (FISBAT). We appreciate the constructive comments offered by R. H. Johns and G. Grice (National Weather Service, Storm Prediction Center) and by the anonymous reviewers, as well as the helpful suggestions offered by the editor, B. R. Colman.

REFERENCES

Barnes, S. L., 1985: Omega diagnosis as a supplement to LFM/MOS guidance in weakly forced convective situations. *Mon. Wea. Rev.,* **113,** 2122–2141.

——, and C. W. Newton, 1986: Thunderstorms in the synoptic setting. *Thunderstorm Morphology and Dynamics,* 2d ed., E. Kessler, Ed., University of Oklahoma Press, 75–112.

Benet, C., 1986: Meteorological data in Sabadell 1897–1979 (in Catalan). 42 pp. [Available from Ajuntament de Sabadell, Pl. Sant Roc 2, 08021 Sabadell, Spain.]

Bolton, D., 1980: The computation of equivalent potential temperature. *Mon. Wea. Rev.,* **108,** 1046–1053.

Buzzi, A., D. Gomis, M. A. Pedder, and S. Alonso, 1991: A method to reduce the adverse impact that inhomogeneous station distributions have on spatial interpolation. *Mon. Wea. Rev.,* **119,** 2465–2491.

Caracena, F., and J. M. Fritsch., 1983: Focusing mechanisms in the Texas hill country flash floods of 1978. *Mon. Wea. Rev.,* **111,** 2319–2332.

Davies-Jones, R., D. Burgess, and M. Foster, 1990: Test of helicity as a tornado forecast parameter. Preprints, *16th Conf. on Severe Local Storms,* Kananaskis Park, AB, Canada, Amer. Meteor. Soc., 588–592.

Doswell, C. A., III, 1987: The distinction between large-scale and mesoscale contribution to severe convection: A case study example. *Wea. Forecasting,* **2,** 3–16.

——, 1994: Flash flood-producing convective storms: Current understanding and research. *Proc. U.S.–Spain Workshop on Natural Hazards,* Barcelona, Spain, National Science Foundation, 97–107.

——, and F. Caracena, 1988: Derivative estimation from marginally sampled vector point functions. *J. Atmos. Sci.,* **45,** 242–253.

——, H. E. Brooks, and R. A. Maddox, 1996: Flash flood forecasting: An ingredients-based methodology. *Wea. Forecasting,* **11,** 560–581.

Durran, D. R., and L. W. Snellman, 1987: The diagnosis of synoptic-scale vertical motion in an operational environment. *Wea. Forecasting,* **2,** 17–31.

Emanuel, K. A., 1991: A scheme for representing cumulus convection in large-scale models. *J. Atmos. Sci.,* **48,** 2313–2335.

Fernández, C., M. A. Gaertner, C. Gallardo, and M. Castro, 1995: Simulation of a long-lived meso-β scale convective system over the Mediterranean coast of Spain. Part I: Numerical predictability. *Meteor. Atmos. Phys.,* **56,** 157–179.

Font, I., 1983: *Climatology of Spain and Portugal* (in Spanish). Instituto Nacional de Meteorologia, 296 pp.

García-Dana, F., R. Font, and A. Rivera, 1982: *Situación Meteorológica durante el Episodio de Lluvia Intensa en el Levante Español durante Octubre de 1982* (in Spanish). Instituto Nacional de Meteorologia, 68 pp.

Hollingsworth, A., D. B. Shaw, P. Lönnberr, L. Illari, K. Arpe, and A. J. Simmons, 1986: Monitoring of observation and analysis quality by a data assimilation system. *Mon. Wea. Rev.,* **114,** 861–879.

Hoskins, B. J., and M. A. Pedder, 1980: The diagnosis of middle latitude synoptic development. *Quart. J. Roy. Meteor. Soc.,* **106,** 707–719.

Lionetti, M., 1996: The Italian floods of 4–6 November 1994. *Weather,* **51,** 18–27.

Llasat, M. C., 1987: Precipitaciones intensas en Cataluña: Génesis, evolución y mecanismo (in Spanish). Universitat de Barcelona No. 40, 543 pp. [Available from Departament de Publicacions, Universitat de Barcelona, Avda. Diadonal 647, 08028 Barcelona, Spain.]

Maddox, R., 1980: Mesoscale convective complexes. *Bull. Amer. Meteor. Soc.,* **61,** 1374–1387.

——, and C. A. Doswell III, 1982: An examination of jet stream configurations, 500 hPa vorticity advection and low-level thermal advection patterns during extended periods of intense convection. *Mon. Wea. Rev.,* **110,** 184–197.

Meteorological Office, 1962: *Weather in the Mediterranean.* Vol. I. Meteorological Office, 362 pp.

Nickerson, E. C., E. Richard, R. Rosset, and D. R. Smith, 1986: The numerical simulation of clouds, rain and airflow over the Vosges and Black Forest mountains: A meso-β model with parameterized microphysics. *Mon. Wea. Rev.,* **114,** 398–414.

Pedder, M. A., 1993: Interpolation and filtering of spatial observations using successive corrections and Gaussian filters. *Mon. Wea. Rev.,* **121,** 2889–2902.

Ramis, C., and R. Romero, 1995: A first numerical simulation of the development and structure of the sea breeze in the island of Mallorca. *Ann. Geophys.,* **13,** 981–994.

——, M. C. Llasat, A. Genovés, and A. Jansá, 1994: The October 1987 floods in Catalonia: Synoptic and mesoscale mechanisms. *Meteor. Appls.,* **1,** 337–350.

——, S. Alonso, and M. C. Llasat, 1995: A comparative study of two cases of heavy rain in Catalonia: Synoptic and mesoscale mechanisms, *Surv. Geophys.,* **16,** 141–161.

Riosalido, R., 1990: Characterization of mesoscale convective systems by satellite pictures during PREVIMET MEDITERRA-

NEO-89 (in Spanish). *Proc. Segundo Simposio Nacional de Predicción,* Madrid, Spain, Instituto Nacional de Meteorología, 135–148.

Romero, R., C. Ramis, and S. Alonso, 1997: Numerical simulation of an extreme rainfall event in Catalonia: Role of orography and evaporation from the sea. *Quart. J. Roy. Meteor. Soc.,* **123,** 537–559.

——, ——, ——, C. A. Doswell III, and D. J. Stensrud, 1998: Mesoscale model simulations of three heavy precipitation events in the western Mediterranean. *Mon. Wea. Rev.,* in press.

Trenberth, K. E., and J. G. Olson, 1988: An evaluation and intercomparison of global analyses from the National Meteorological Center and the European Centre for Medium-Range Weather Forecasts. *Bull. Amer. Meteor. Soc.,* **69,** 1047–1057.

Tudurí, E., and C. Ramis, 1997: On the environments of significant convective events in the western Mediterranean. *Wea. Forecasting,* **12,** 294–306.

Weisman, M. L., and J. B. Klemp, 1986: Characteristics of isolated convective storms. *Mesoscale Meteorology and Forecasting,* P. S. Ray, Ed., Amer. Meteor. Soc., 331–358.